2015

Examination of the effects of external load, velocity, and center of gravity on weight estimation using a lifting linkage

Ryan McCleish
Iowa State University

Examination of the effects of external load, velocity, and center of gravity on weight estimation using a lifting linkage

by

Ryan McCleish

A thesis submitted to the graduate faculty

in partial fulfillment of the requirements for the degree of

MASTER OF SCIENCE

Major: Mechanical Engineering

Program of Study Committee:
Judy M. Vance, Major Professor
Greg R. Luecke
Brian Steward

Iowa State University

Ames, Iowa

2015

TABLE OF CONTENTS

LIST OF FIGURES iii

LIST OF TABLES v

ABSTRACT vi

CHAPTER 1: INTRODUCTION 1

CHAPTER 2: BACKGROUND 4

2.1 Background of weight measurement 5

2.2 Weighing methods 9

2.3 Related work 12

CHAPTER 3: METHODS 16

3.1 Theoretical model 20

3.1.1 Model development 20

3.1.2 Software simulation 24

3.2 Experimental setup 25

3.3 Testing procedures 28

CHAPTER 4: RESULTS 32

4.1 Static load 32

4.2 Constant velocity 35

4.2.1 Varying load 37

4.2.2 Varying velocity 38

4.2.3 Varying center of gravity 39

4.3 Combined theoretical and experimental results 40

4.4 Experimental error 42

CHAPTER 5: DISCUSSION AND CONCLUSIONS 47

BIBLIOGRAPHY 50

ACKNOWLEDGEMENTS 53

LIST OF FIGURES

Figure 1: An image of an early Egyptian balance scale is painted on a tomb. 6

Figure 2: A triple beam balance setup, where the weight is placed on a plate on the left and the three weights on the right are moved to bring the system to balance. 7

Figure 3: A pressure transducer can be used to read the pressure change due to a force, F, applied to a piston [14]. 9

Figure 4: A weighing conveyor can be used to measure the weight of a package in motion. 12

Figure 5: A four axle truck carrying a payload would require sensors on each axle. 13

Figure 6: Linkage used on a front loader used to transport bulk material. 14

Figure 7: A material moving machine with a multipart linkage that consists of 3 cylinders and a bucket. 15

Figure 8: (a) The four links of the arm assembly are listed on a side view. (b) An isometric view shows the full linkage. 18

Figure 9: (a) The top picture shows the arm and fork cylinders extended and (b) the bottom image shows both cylinders fully retracted. 19

Figure 10: The position vectors are shown on top of the arm linkage. 21

Figure 11: The external force vectors at P1 and P2 are forces exerted by a pin, and Fm is the force of an external load on the fork. 22

Figure 12: The forces for a generic link are shown, with an external force F. 23

Figure 13: The test system is shown with both the arm and fork cylinders fully retracted and the two inclinometer locations shown. 25

Figure 14: The left cylinder shows retraction, while the right cylinder shows extension. The red represents high pressure and the blue low pressure. 26

Figure 15: The fork angle sensor on the left and the arm angle sensor on the right were used to measure the angles of each cylinder. 27

Figure 16: The varied CG for the weighted container can be seen at L1, L2, and L3 29

Figure 17: A top view of the container is shown, with CG_1, CG_2, and CG_3 running down the center of the container and CG_4 offset to one side of the container. 30

Figure 18: The force results of the arm cylinder were measured for no load (0 pound), medium load (3,300 pounds), and heavy load (5050 pounds). 33

Figure 19: The force results of the fork cylinder were measured during no load and medium load (3,300 pounds) conditions. 34

Figure 20: The force results of the arm cylinder were measured at a static position and no addition weight, during arm raise and lower. 34

Figure 21: The force results of the arm cylinder were measured at constant velocity and no additional weight, during arm raise and lower. 36

Figure 22: A moving average is overlaid on top of the raw data collected. 36

Figure 23: The force results of the arm cylinder were measured at constant velocity for three different loads: heavy (5,050 pounds), medium (3,300 pounds), and no load (0 pounds). 37

Figure 24: The force results of the arm cylinder were measured at four different arm speeds, which were stopped (0 deg/s), low (3.5 deg/s), medium (7.4 deg/s), and high (12.4 deg/s) speeds. 38

Figure 25: The force results of the arm cylinder were measured at medium weight (3,300 pounds), for the three different front to back CG locations. 39

Figure 26: The force results of the arm cylinder were measured at medium weight (3,300 pounds) for the two lateral CG locations. 40

Figure 27: The experimental force was measured at the arm cylinder and compared to the theoretical results. 41

Figure 28: The experimental force data was measured at the arm cylinders in constant motion and compared to the theoretical results, during arm raise and lower. 42

Figure 29: The mechanical advantage of the cylinder and external load are shown relative to the pivot point P2. 43

Figure 30: The error between the theoretical and experiment load was compared, for the varying load data. 45

Figure 31: The error between the theoretical and experiment load was compared, for varying velocity. 45

Figure 32: The error between the theoretical and experiment load was compared, for varying center of gravity. 46

LIST OF TABLES

Table 1: The external load placed on the forks ranged from 0 to 5050 pounds. 28

Table 2: The angular speed of the arm link ranges from 0 to 12.4 degrees per second, and the container linear speed varies from 0 to 2.5 ft/s. 29

Table 3: The list shows the summary of conditions for each of the tests performed. 30

ABSTRACT

Having an accurate measurement of the weight of a vehicle payload is important, when moving material. An accurate knowledge of the payload can increase efficiency during material transportation, by ensuring the maximum payload is being moved. Many existing weight measurement systems exist but are often costly, add significant weight, or increase operating time. An improved dynamic weight measurement system to estimate the weight of a payload inside of a container is proposed in this research. Using pressure transducers and angle sensors on a lifting linkage, the weight of a payload is calculated in constant motion, which minimizes any time loss due to measurements. A math model was developed, and the results were simulated to determine the major contributing factors that affect the pressure. An experimental setup was used to test the effects that pressure has on three variables: velocity, center of gravity, and weight. The results showed that each of the experimental variables could be independently varied and had an effect on the cylinder pressure.

CHAPTER 1: INTRODUCTION

The ability to measure a weight in motion is important in many industries. Having an accurate weight measurement is especially important for vehicles transporting a payload. Many existing measurement systems take readings of a payload picked up by a vehicle at a stopped position. More advanced systems can weigh a vehicle and payload while the vehicle is stopped and the payload is in motion; however, these systems either add significant weight or cost to the vehicle. There is a growing need for an on-board dynamic payload weighing system that is lightweight and lower cost.

Knowing the weight of a vehicle and payload can improve the efficiency and reduce the time required to move a payload. If a vehicle is underloaded, it is inefficient and can consume unnecessary energy by requiring more fuel to move a given total load. Overloading can be even more detrimental, resulting in a reduction in the life of a vehicle and potentially violating load regulations, which can result in fines. There are many advantages to weighing a payload in motion. Depending on the measurement technique used, waiting for sensors to reach steady state can be time consuming. As minimizing time is often a critical requirement, taking measurements while stopped can lead to unwanted added time [1]. The extra time is due to the time required to come to a stop and waiting for the weight sensors to achieve a steady state value. Weighing the vehicle in motion removes takes less time and improves efficiency of the operation.

Measuring the weight of an object has been a common practice throughout history. However, until recent years inexpensive and effective dynamic weight measurement sensors had not been developed [2]. As sensor technologies have advanced, more cost effective and reliable systems have been created in many industries, including the material transportation industry.

In vehicle material transportation there are a number of ways to measure vehicle weight. Common devices include truck scales, which are used at weigh stations. These scales weigh vehicles either stopped or in motion. When a vehicle's weight is frequently changing, on-board scales become necessary. On-board scales are common in the refuse, mining, and agricultural industries, among others. Some applications for on-board weighing include load cells and sensors to measure the chassis axle deflection.

The research in this paper suggests a method of measuring the weight for a payload inside a container that is being moved by a linkage attached to a vehicle. Using pressure transducers and angle sensors on a linkage, the weight of a payload is calculated throughout the dumping motion. The difference between the full and empty container can be used to determine the payload weight inside the container. The technique of using sensors to estimate the dynamic payload is quick and minimally invasive, requiring minimal interaction from an operator and adding little or no operation time. In static measurements sensors must achieve steady state before an estimation can be made. Once the measurements are gathered, additional more complex calculations can be performed, if real time results are not required.

In this paper a theoretical model is developed for a linkage system used on a refuse front loader; however, the theory can be generalized for other linkages. This model is used to compare theoretical data versus empirical measurements taken. The model and data will be used to determine the major contributing factors used in determining the weight. During testing, linear actuator pressure and angle sensors will be used to determine the forces in the system, which can be used to estimate the unknown weight. The factors to be varied during testing are velocity, center of gravity, and weight. Initially, a static model is presented and compared to measured data. A constant velocity model is also presented and compared to empirical data. The

measured data is compared to a simulation based on the theoretical model, which calculates values at multiple points.

The remainder of this thesis is organized as follows: Chapter 2 provides background information and research, Chapter 3 outlines the theoretical model and experimental methods, Chapter 4 presents the results from the theoretical model and experimental results, and Chapter 5 discusses the results and suggests direction for future research.

CHAPTER 2: BACKGROUND

Material transportation plays an important part of many industries. In particular waste collection affects people in the United States and around the world on a daily basis, both in residential and commercial settings. Each year people throw away millions of tons of refuse, or municipal solid waste (MSW). In 2012 the United States produced over 250 million tons of refuse annually, which equates to over 4 pounds a day per person [3]. Of this about 34.5% is a recycled and composted material.

Reliable weight monitoring is an essential piece of the material transportation process. Commercial vehicles are often required to stop at weighing stations for inspection to verify the weight is in compliance with current regulations. Maximizing the amount of material in the truck up to the extent of the law is the most efficient use of the truck. By using the truck to its maximum capacity, operation time and fuel consumption can be reduced. In addition, the truck will have a much more predictable and consistent payload, which can be useful for route planning.

There are several drawbacks to not having an optimal payload. Too much weight being transported can overload the truck, which can be damaging and reduce system life. Overweight vehicles even violate the law, which can result in penalties and fines [4]. The responsibility for ensuring the vehicle is in compliance falls on the driver. This can encourage the driver to be conservative in the amount of material loaded into a truck. Underweight vehicles can increase the overall costs, by increasing the driving time and fuel consumption, requiring additional trips to move all of the material. Partial loads underutilize the system, which lowers the process and system efficiencies. This increases operation time and increased fuel costs. Both of these factors

cause an increase in total cost. An optimized load can reduce fuel consumption and increase the amount of material transported in a given time.

Because of the difficulty in maximizing the load, while not overloading the vehicle, many vehicles are equipped with on-board weight measurement and monitoring systems. These systems aid the driver, improving the efficiency and consistency of the payload. However, many of these systems have downsides, having either a high cost or noticeably increasing the overall system weight. There is a growing need for a system that is lightweight and cost effective.

2.1 Background of weight measurement

The first known scales were used nearly 6,000 years ago [7], [8]. Egyptians paintings of scales used for weighing can be seen in **Figure 1**. These scales had both religious symbolism and practical uses for ancient Egyptians. During this time period, scales were often used to measure precious stones or items for commerce. The Egyptian scale functioned by using known reference weights. Pans, used to hold the object being weighed and the reference weights, were suspended from either end of a beam. The object being weighed was placed on the pan on one side of the balance beam, while known reference weights were put on the opposite side of the beam and adjusted until equilibrium is achieved. To account for the challenge of getting the scale exactly balanced, a vertical pointer was added at the fulcrum to determine accuracy, by displaying the error from perfect balance. This setup was a basic version of a balance scale, which is still used today. While simple, the scale developed by the Egyptians was effective and was the main scale in use for thousands of years.

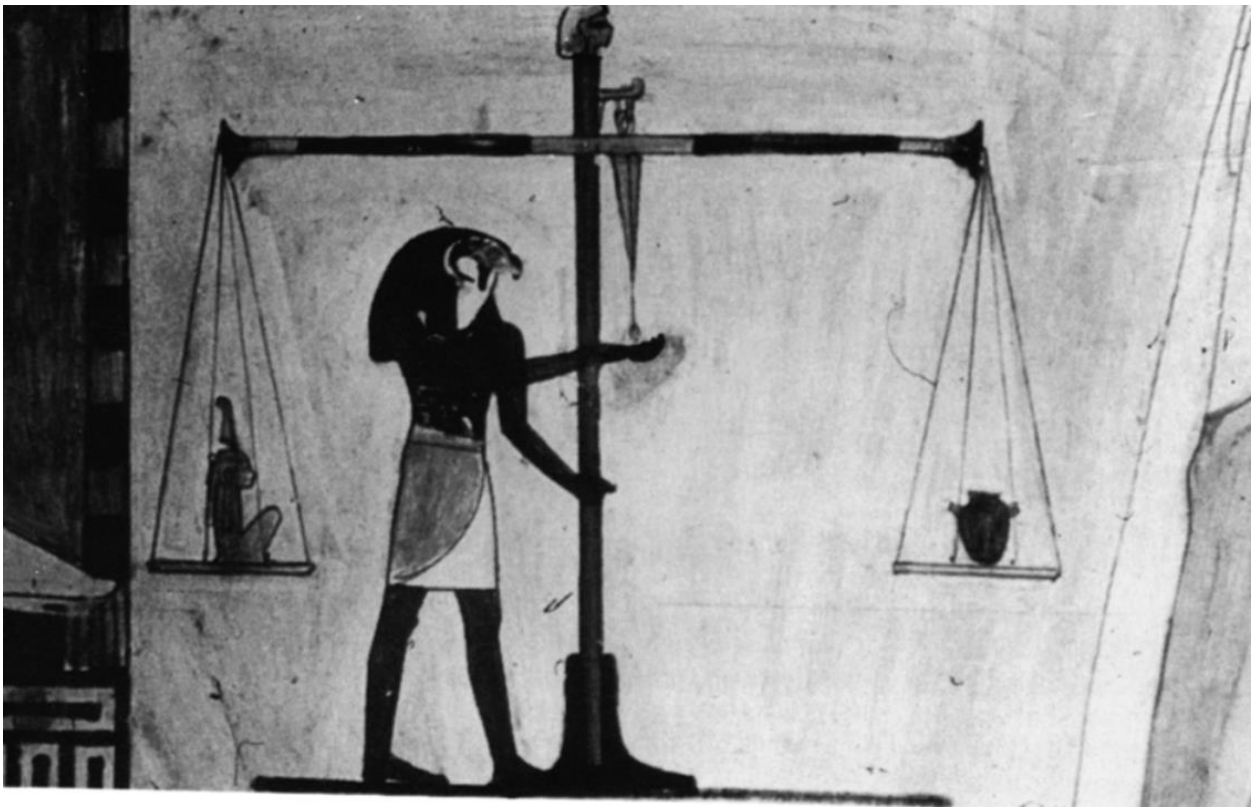

Figure 1: An image of an early Egyptian balance scale is painted on a tomb.

The basic principles used in the original balance beam have been critical to the development of many scales used in the past and present. While simple, the idea of bringing two objects into an equilibrium balance is still in use. Using reference weights is an easy and effective way to quickly estimate the weight of an object. The next major development in weight scales came as a modification to the original balance scale. The new scale relied on varying the length of the moment arm, instead of using multiple reference weights. The setup still relied on placing weights on a similar style balance; however, once the reference weight and object being weighed were placed on the balance, the balance beam could be shifted from side to side relative to the fulcrum. In shifting the balance beam to one side, the length of beam to the unknown weight could be shortened or lengthened to achieve balance with a reference weight. By varying

the length of the moment arm from the fulcrum to the unknown weight, a single reference weight could be used for a range of unknown object weights.

Several thousand years after the balance scale was developed, another important scale that came about was used in many countries. It is called the steelyard scale, or Roman staterae, among other names [9]. Using the steelyard scale, a weight is placed on a hook on one end, while a known weight was slid across a beam. This motion varied the length of the lever arm. The principles used in this scale can still be seen in the triple beam balance, often used today [10], [11].

In a triple beam balance assembly three moveable weights are allowed to slide along one side of the balance as seen in **Figure 2**, while the weight to be measured is placed on a plate on the opposite side of the fulcrum. The three moveable weights can be moved to nominal locations, with the three weights representing different magnitudes. The heaviest weight is moved first and the fine weight last. The needle on the right side moves up and down as the weight is varied. A balance is achieved when the needle points to the middle, which is often marked for easy identification.

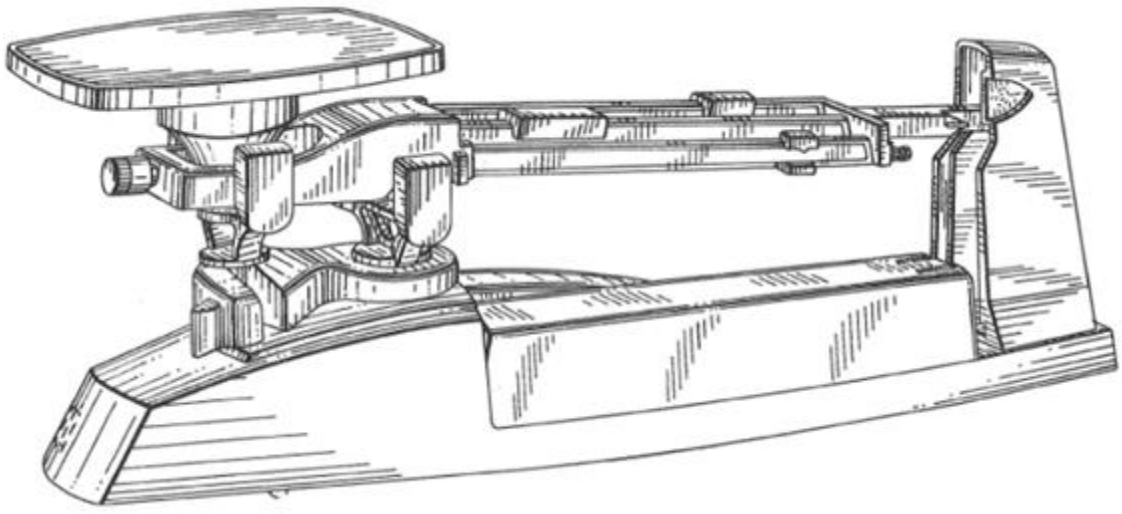

Figure 2: A triple beam balance setup, where the weight is placed on a plate on the left and the three weights on the right are moved to bring the system to balance.

While slight improvements and variations of scales continued for thousands of years, significant new ideas were not introduced until the 15th and 16th centuries. The work of Leonardo Da Vinci is the basis for many scales used today [12]. He investigated the lever system, which led to the development of a number of scales, like the lever platform scale. In addition he developed the first dial indicator and introduced techniques to improve the accuracy of scales. He even sketched and described a system, similar to the spring balance, which wasn't invented until centuries later by Hooke. The spring scale uses the principles of Hooke's law. For a known spring stiffness, the distance can be measured and used to calculate the force or weight applied [13].

Perhaps one of the most significant advancements in weight measurement technology came in 1938, when Arthur Ruge developed the bonded wire strain gauge [2]. This strain gauge was the first weight measurement tool that did not require a physical force balance. Instead it relies on measuring the electrical resistance of deformed wire. Today, the strain gauge remains one of the most common weight measurement tools, being used in many measurement devices.

Within the last century the development of load cells continues to improve weight measurement, providing a unique way to take weight measurements using a hydraulic system [12]. Pressure measurements can be obtained from the system and used as a tool for determining the weight of an object. The basic principles are illustrated in **Figure 3**. A system with a known pressure is read on a pressure gauge or pressure transducer. A force is applied to the piston, which increased the pressure of the system. Then, the pressure can be used to calculate the force applied.

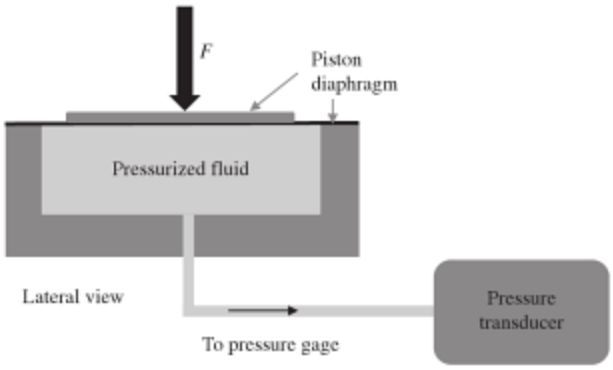

Figure 3: A pressure transducer can be used to read the pressure change due to a force, F, applied to a piston [14].

2.2 Weighing methods

Mass measurements are currently being used for calculating masses of all sizes. New methods are constantly being developed to measure masses from quarks [15], [16] to planets [17]. These continue to stretch our ability to better understand and quantify the world around us. More common techniques continue to be applied in new ways every day. Many of these applications are used regularly. Some applications of modern measuring techniques include high precision instruments, static scales, and dynamic scales.

Since the development of strain gauges, the increased accuracy of measuring devices has allowed easier access to more precise measurements. Whereas good precision measurements can be made with the triple beam scale, the scale is somewhat complex. The invention of strain gauges made force measurements simpler and more accurate [18]. Strain gauges are commonly used today, when electronically measuring pressure, force, and displacement, among other physical properties. While strain gauges continue to be one of the most dominant force measurement tool used, at very high precision even these gauges can become susceptible to environmental effects.

Today weight can be found to a very high accuracy in a laboratory setting, both statically and dynamically [19]. In the laboratory case, controlling many factors such as dust contamination, temperature, humidity, and atmospheric pressure becomes important, since the error caused by these quantities have a greater impact at higher accuracy. Making similar measurements outside of the laboratory setting is not possible because of the effect that these factors have on the measurements and the inability to control the factors to the degree necessary to produce highly accurate readings.

Static weight measurements are a common way to measure the weight of an object, which can be used to measure a stationary object. Examples include objects set on a bathroom scale or a food scale [20] . Many bathroom scales use strain gauges, which involve measuring the change in distance of the gauge [21]. In the past, bathroom scales commonly used a spring balance to estimate the weight of a person. The springs are calibrated at particular weights, so that the entire range is within the desired tolerance. As a weight or force is applied to the scale, the springs compress and the calibrated weight is displayed. Many digital bathroom scales and other modern scales use strain gages in place of springs. Strain gauges allows for compact sensors to be used to measure with high accuracy [18].

Dynamic weight measurement requires measuring the velocity and acceleration of a weight in addition to its change in distance. Sensors collect information about the dynamic movements of the system. The impact of force from the weight is measured through sensors, such as strain gauges or pressure transducers. Once the readings are taken, an algorithm is used to estimate the weight of the object being measured.

A critical part of dynamic weight measurement systems is to obtain accurate measurements at sufficient measurement speeds. In a paper by Ono et al., he describes this

challenge and proposes a way to improve electronic scales, by using a method to quickly and accurately measure an object's weight [1]. He goes on to suggest a way to improve the scale is through estimation techniques [23], [24]. Three techniques were compared: static measurement, dynamic measurement with a linearly approximated system, and dynamic measurement with a non-linear system. Using a non-linear system with a filter was the most accurate; however, non-linear systems require more processing power, making the use of any real time application difficult. The linear system with a Kalman filter was also fairly accurate. In addition, it reduced the measurement time and required minimal processing time, which suggests the filter is a more suitable choice for real time measurement applications. In order to achieve the accuracy of the non-linear system without using a large amount of processing power, using additional experimental data, initial parameters and linear approximations proved to be a feasible approach to achieving high accuracy, while reducing the time to calculate the weight [25].

In a paper by Pietrzak et al., a checkweigher system is described, which is a common dynamic weight measurement device used for measuring packages on conveyors [22]. A key advantage to the checkweigher weight measurement system is its minimal invasiveness, during the transportation of the packages. The contents of the packages can vary and are unknown. The system is automated, requiring no operator involvement to run the machine.

The measurement instruments for the checkweigher consist of a weighing sensor and a transport system, i.e., the conveyor. **Figure 4** shows a picture of the basic conveyor setup. A package of weight m and length l is measured, while moving at velocity v across the weighing conveyor of length L [22]. Continuous measurements are taken of the package as it moves across the weighting conveyor. From here the package continues onto additional non-weighing conveyors. The measurements taken are then used to estimate the weight of the package or

object. Like many non-laboratory applications, sufficient accuracy (1% or better) can be achieved by approximating environmental conditions such as temperature and humidity. Here, the major system error comes from mechanical vibrations. Pietrzak et al. discusses using one or more low-pass filters on the data measurements to get rid of much of the variation in the results due to the mechanical vibrations and get adequate weight measurements.

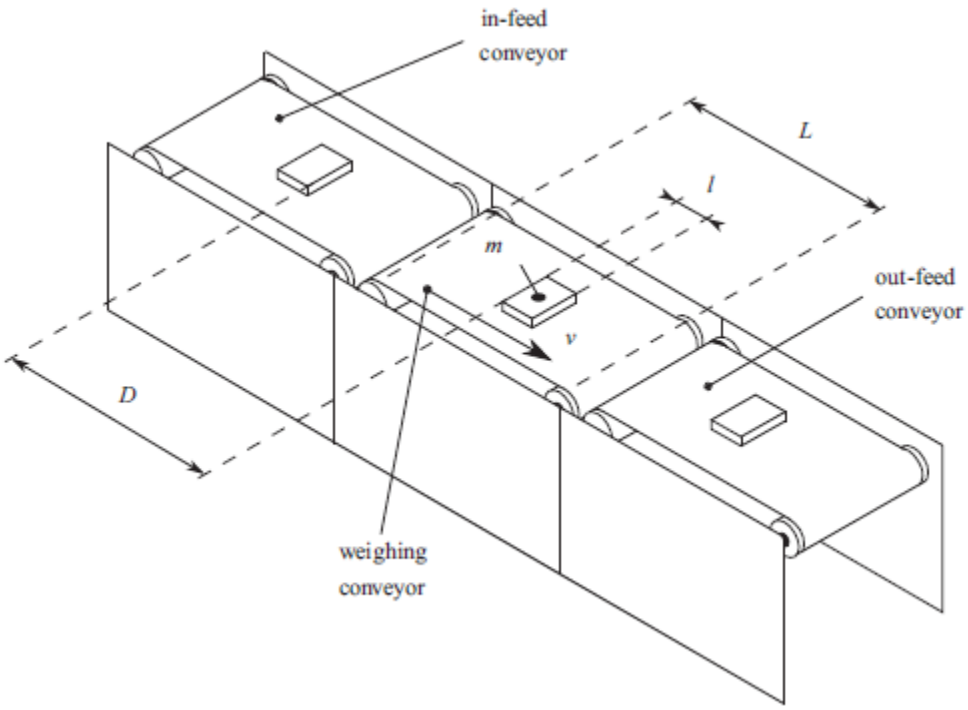

Figure 4: A weighing conveyor can be used to measure the weight of a package in motion.

2.3 Related work

Applications for the research presented in this thesis include mobile equipment. There are many methods that are used for weighing objects carried by mobile equipment. Many regulations require trucks or other mobile equipment to limit the weight of a load as these are often the criteria that the roads themselves are designed to meet [26], [27]. These regulations require that trucks are regularly weighed and impose penalties when these regulations are not

followed, which demonstrate the importance of not overloading vehicles. However, in order to minimize the time lost due to constantly measuring a truck or load, there are systems that measure the weight of the truck in motion. While these on-board weight systems are not acceptable for an official regulated weigh in, these assist the driver in filling the truck to an optimal load.

One method for measuring the weight of a truck in motion is to measure the displacement of either the suspension or axle of a truck [28]. Measurements can be attained by attaching a sensor to each of the axles of a truck [29]. The sensor measures the deflection of each axle, which is used to estimate the weight on each axle (and gross vehicle weight) from the initial calibration. As seen in **Figure 5** sensors can are placed at each axle, represented by numbers 25, 30, 35, and 40. The weight estimates from each axle are added up to give a total estimate of the weight of the truck. Additional equations are often used to take various environmental conditions and assumptions into account.

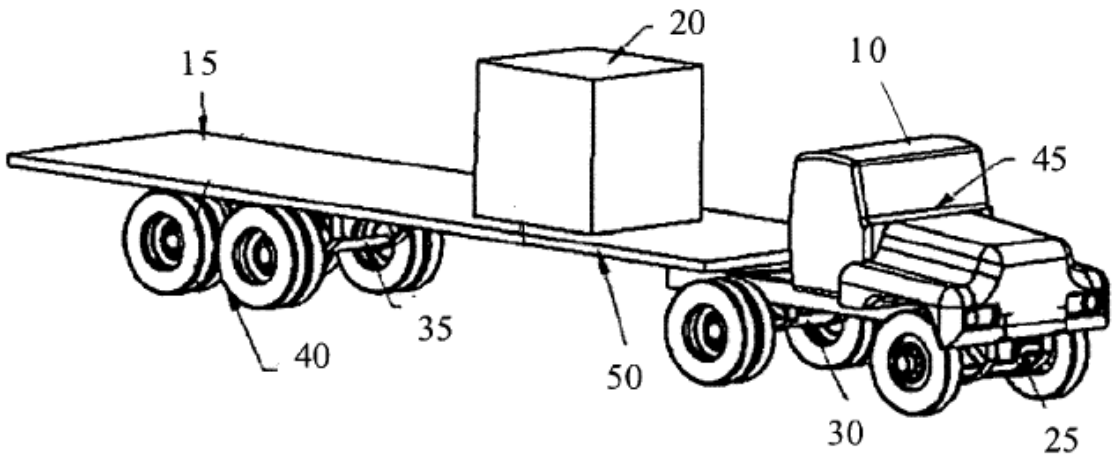

Figure 5: A four axle truck carrying a payload would require sensors on each axle.

Using axle and suspension deflection measurements for weight estimation is growing in popularity. These techniques require a fixed amount of sensors per axle and are general enough to accommodate a variety of trucks. As previously mentioned, a dynamic weight measurement requires velocity and acceleration measurements in addition to distance. The weight of a truck shifts during acceleration, turning, etc. These motions can cause errors in the measurements. The error can be minimized by using additional sensors or estimations in the algorithms.

Another technique used in commercial truck dynamic weight measuring is to utilize load cells [30]. With this technique, the weight of a chassis payload is supported on a set of load cells. With the accompaniment of accelerometers, the load cells can measure the weight of the payload in motion. Again an algorithm estimates the total weight and how it is distributed. The drawback to using load cells is the significant weight that is often added.

Vehicle payload monitoring is common in transferring of bulk material. **Figure 6** and **Figure 7** show two different linkages used for bulk weight transfer. The weight of the material being lifted is measured, using sensor information.

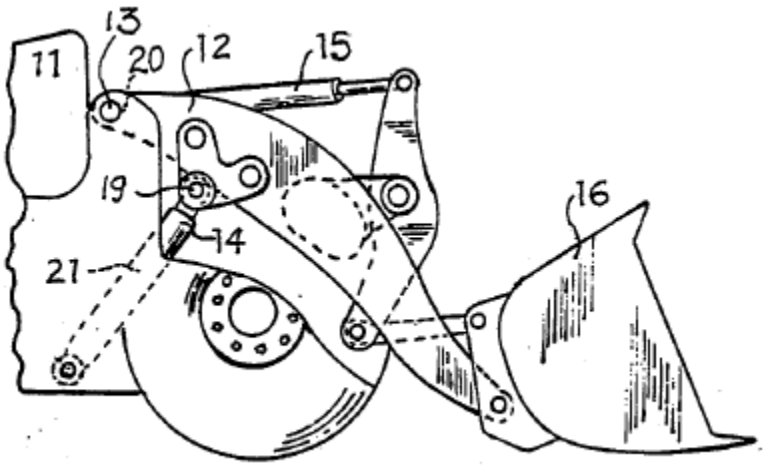

Figure 6: Linkage used on a front loader used to transport bulk material.

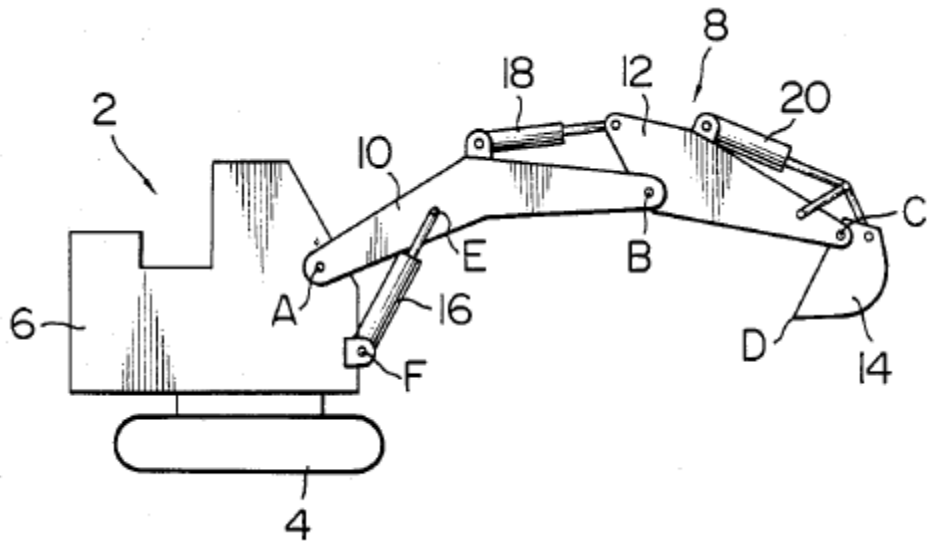

Figure 7: A material moving machine with a multipart linkage that consists of 3 cylinders and a bucket.

Figure 6 shows a front bucket loader that is used for moving bulk material [31], and **Figure 7** shows a machine for moving material [32]. These are common machines used on construction sites today. Both machines consist of a linkage with hydraulic linear actuators and a bucket. Sensors are used to measure change in hydraulic pressure and change in geometric angles. An algorithm is used to estimate the weight of material being moved.

The algorithm for the front loader machine in **Figure 6** uses curve fitting to approximate the payload from measured pressures. Minimum and maximum values are set based on empirical data from a no load and known load scenarios. Data is interpolated from these values, but can also be extrapolated to some extent. The algorithm in **Figure 7** relies on the kinematics of the machine in addition to the sensor data to estimate the weight of material being lifted.

CHAPTER 3: METHODS

The goal of this research is to determine the factors that effect cylinder pressure in a particular linkage and evaluate the impact that the factors have on the pressure. This research is an initial investigation to develop and validate a simple technique for estimating an unknown weight inside of a container that is being lifted by a linkage. Beyond validation, the testing is used to determine the main variables in the system that affect the actuation force. A linkage is used to move the container and weight. During operation, the container and unknown weight are lifted, then the weight is dumped out of the container, and the empty container is lowered. Cylinder pressure sensors and angle sensors are used to record data. When the cylinder pressures and link angles are used as the inputs, the weight of the container is estimated. Conversely, for a fixed weight, the pressure can be recorded at different cylinder angles to estimate an external load. A theoretical model was developed to determine what the major contributing factors that affect the pressure were. Variables used in the tests included container weight, center of gravity of the payload and velocity of the payload. The effects these variables have on the cylinder pressures are recorded. Results from an experimental test setup are used to determine how these factors affect the pressure.

Using many of the same principles of early scales, a non-traditional shaped scale can be created to weigh an object with unknown properties in a container. **Figure 8** illustrates the linkage that will be the focus of this research. It is a lifting linkage that is used on a front loader refuse truck. A container can be picked up by link 4. Placing a weight on the forks causes an increase in pressure in each of the two hydraulic cylinders. The relationship between the two pressures and the weight can be used to calculate the weight on the end of the forks at known link angles.

The goal of testing is to determine a relationship between the pressure and the container weight, for different container weights, locations, and velocities.

Figure 8(a) shows the links used in the model and experimental setup, and **Figure 8(b)** shows the isometric view. Each link represents a pair of identical links that make up an arm subassembly. The entire linkage consists of two identical subassemblies, separated by two tubes: one tube connecting P2 on each subassembly and the other tube connection P5 on each subassembly. Since the subassemblies are identical, only one will be used for the analysis in this research.

The system consists of four links, where links 1 and 3 are hydraulic cylinders and the remaining two links are fixed. The global x and y axis are shown at the origin. P1 and P2 are fixed to the truck frame. Link 1 pivots about P1 and Link 2 pivots about P2. P5 connects Link 2 to Link 4. P6 connects Link 3 to Link 4. P5 and P6 are part of the rigid Link 4 and therefore have no relative movement between them. Link 1 and Link 3 are individually actuated. A container is fixed to a location along link 4.

Link 1 will also be referred to as the arm cylinder and link 2 as the arm. Link 3 will be referred to as the fork cylinder and link 4 the fork. Links 1 and 2 form the subassembly called the arm assembly, and links 3 and 4 form the fork assembly.

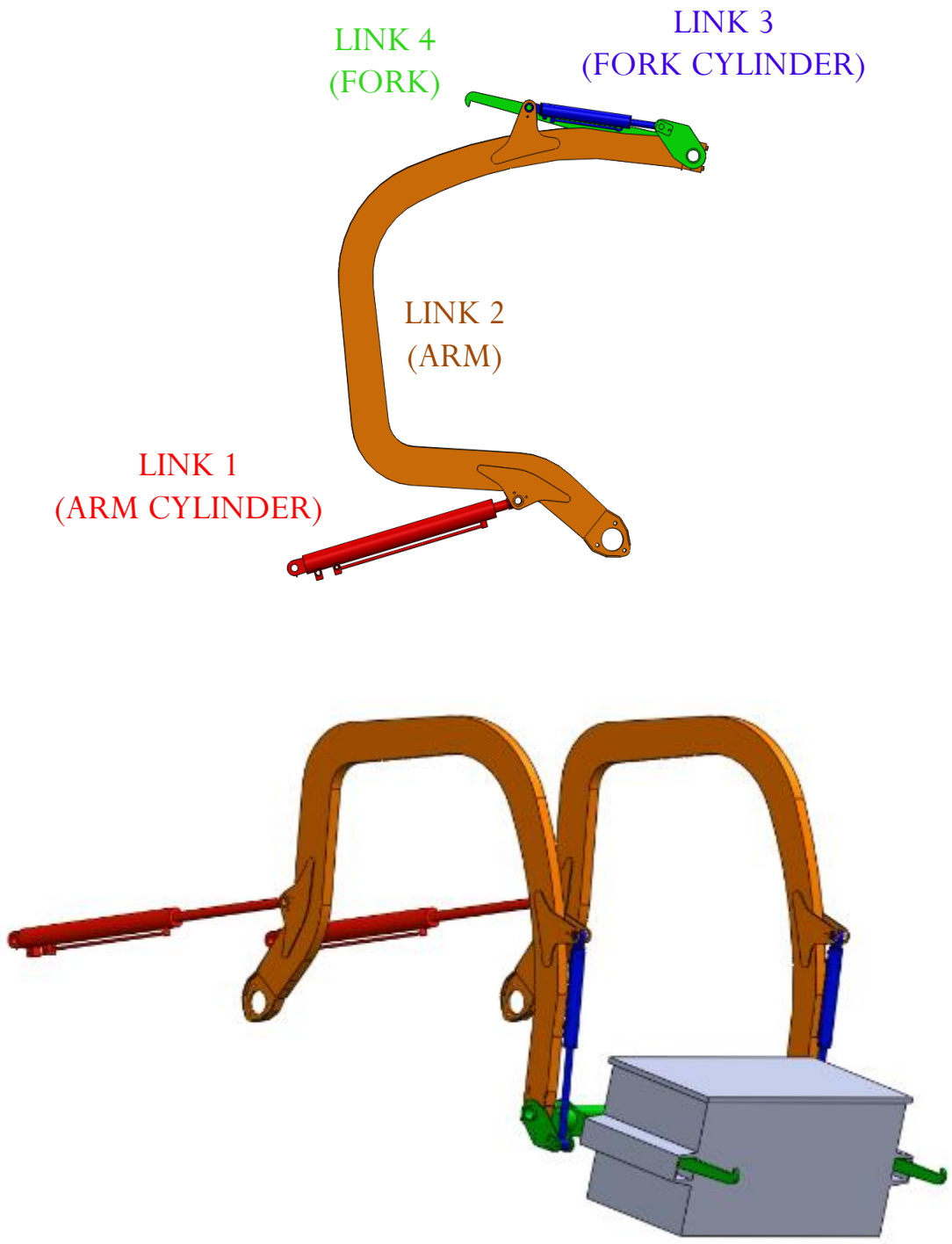

Figure 8: (a) The four links of the arm assembly are listed on a side view. (b) An isometric view shows the full linkage.

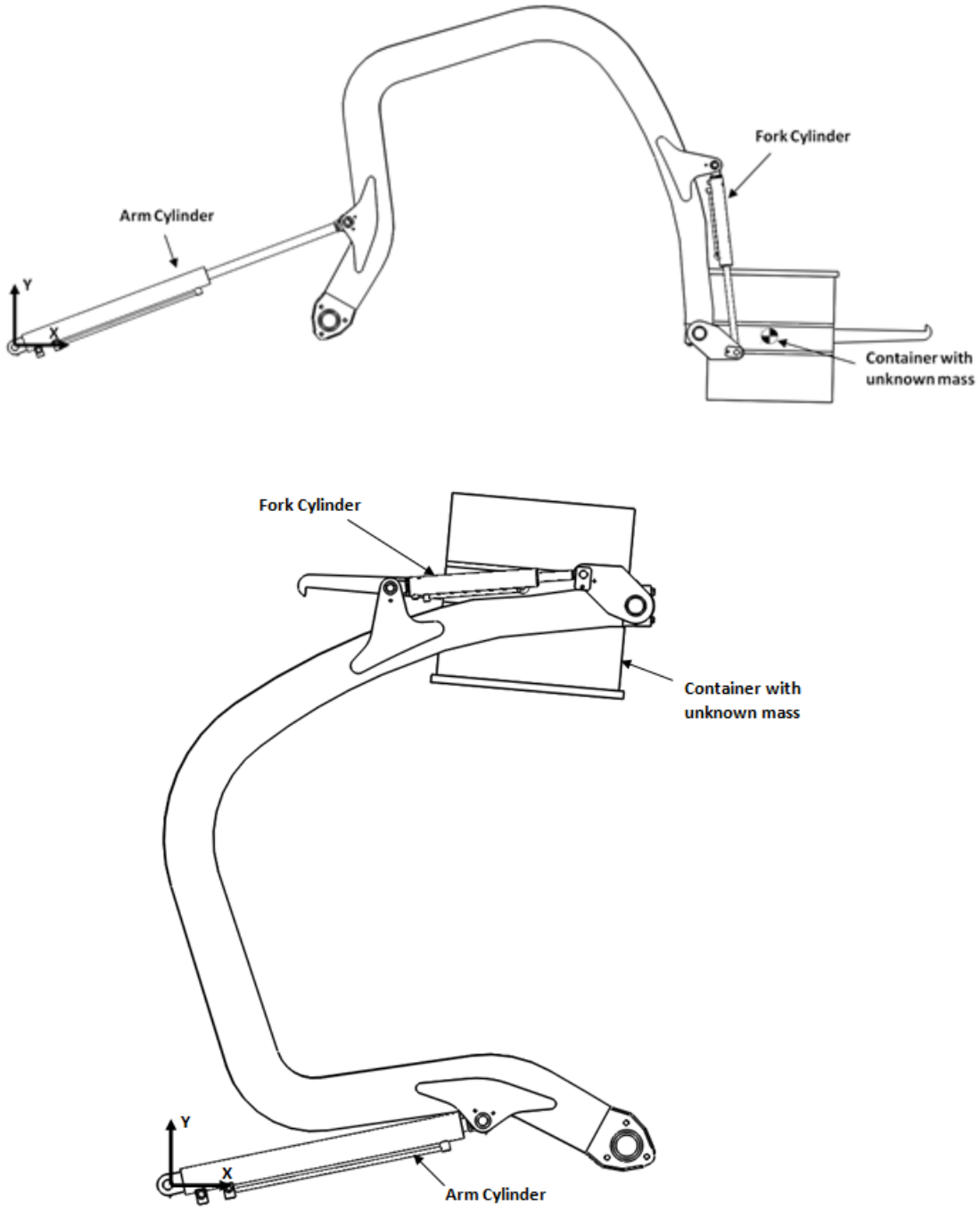

Figure 9: (a) The top picture shows the arm and fork cylinders extended and (b) the bottom image shows both cylinders fully retracted.

During the linkage motion an unknown weight inside a container is picked up and rests on the fork assembly as seen in **Figure 9a**. When the arms reach their lowest point, the two arm

cylinders are in the fully extended position. As the two arm cylinders are retracted, the fork cylinders are also retracted independently causing the container to gradually dump its content into the truck as seen in **Figure 9b**. Finally, the cylinders are extended to return the empty container to the ground, and then the forks are removed. A theoretical model is developed and experimental results are obtained and compared to the theoretical model.

3.1 Theoretical model

A theoretical model was developed for the linkage system seen in **Figure 9**, where the container and unknown weight are represented by an external force at the center of gravity of the container. A simulation was used to solve the theoretical model for cylinder forces at a number of arm and fork cylinder angles, for a particular weight.

3.1.1 Model development

The math model was used to calculate the theoretical forces seen at the cylinders. **Figure 10** shows the position vectors used for the models, overlaid onto a model of the linkage system used.

The vector subscripts represent the tail and head ends of the vector respectively. For example, $\mathbf{R_{13}}$ is the vector with the tail at point 1 and the head at point 3. Note that $\mathbf{R_{13}}$ and $\mathbf{R_{46}}$ represent the two linear actuators. Since the lengths of the remaining links do not change shape or size, by determining the length and angle of these two vectors the position of every point on the linkage is known. P_m is the center of gravity for the external force from the container.

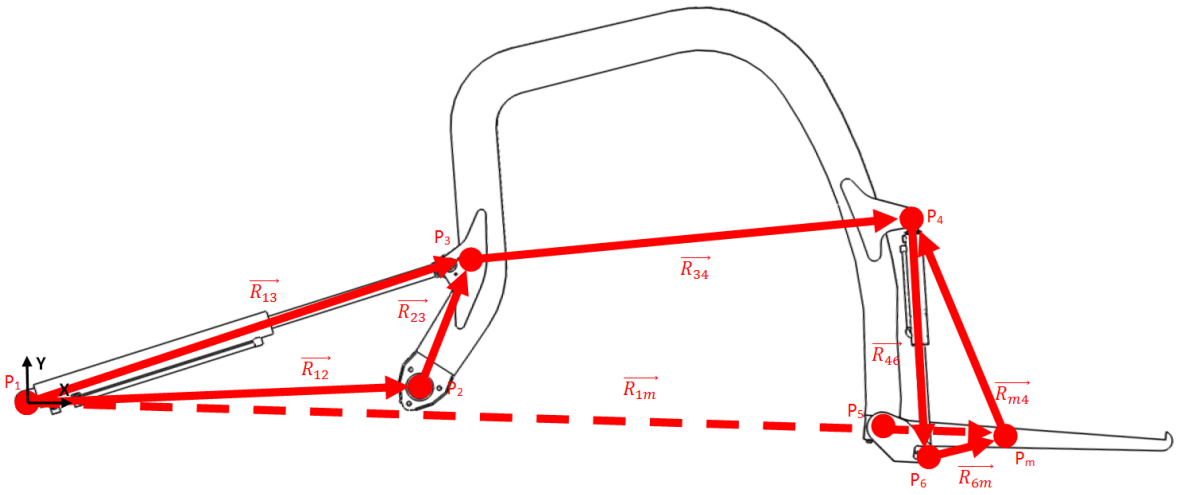

Figure 10: The position vectors are shown on top of the arm linkage.

The two actuator vectors can also be represented by the sum of two vectors that form a triangle. This can be seen in **equations (1)** and **(2)**. Likewise, we can write the velocity vectors in the same way, which can be seen in **equations (3)** and **(4)**.

The position and velocity equations for the center of gravity of the container can be written from these vectors as a function of the two actuators as seen in **equations (5)** and **(6)**. Vector $\mathbf{R_{34}}$ is a fixed length offset, and $\mathbf{R_{6m}}$ is the distance from the end of the fork cylinder rod to the center of gravity of the external force.

$$R_{13} = R_{12} + R_{23} \quad \textbf{(1)}$$

$$R_{46} = -(R_{6m} + R_{m4}) \quad \textbf{(2)}$$

$$\dot{R_{13}} = \dot{R_{12}} + \dot{R_{23}} \quad \textbf{(3)}$$

$$\dot{R_{46}} = -(\dot{R_{6m}} + \dot{R_{m4}}) \quad \textbf{(4)}$$

$$R_{1m} = R_{13} + R_{34} + R_{46} + R_{6m} \quad \textbf{(5)}$$

$$\dot{R_{1m}} = \dot{R_{13}} + \dot{R_{34}} + \dot{R_{46}} + \dot{R_{6m}} \quad \textbf{(6)}$$

The external forces on the linkage are shown in **Figure 11**. These are the forces exerted from the environment or attached components onto the linkage. $\mathbf{F_1}$ is the resultant force onto the

pin at the base end of the arm cylinder. $\mathbf{F_2}$ is the resultant force exerted onto the pin at the pivot point of the arm link. Both forces are shown broken down in the x and y components. Force F_m is the force exerted by the center of gravity of the container.

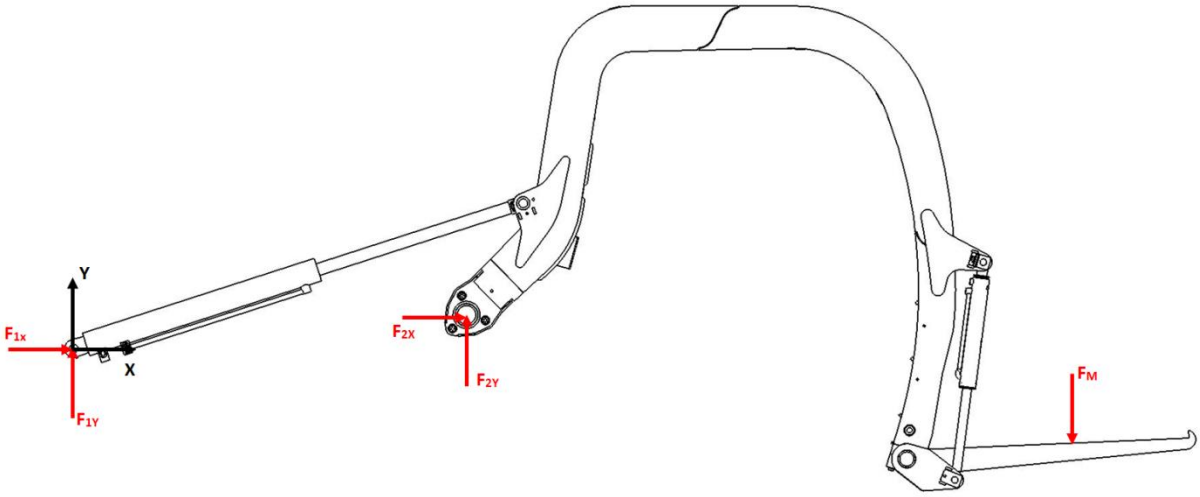

Figure 11: The external force vectors at P1 and P2 are forces exerted by a pin, and Fm is the force of an external load on the fork.

To examine the system and determine the relationship of these forces and how they relate to the pressures of the cylinders requires an analysis of each link. A generic free body diagram for a link is shown in **Figure 12**.

The link shows forces at the two endpoints P_1 and P_2. An external force $\mathbf{F_{external}}$ is used for any external forces, such as the container or environmental factors; however, the only external force that will be considered in this system is the container and the payload weight inside of it. The weight of the link is represented as $\mathbf{F_g}$ at the link's center of gravity. The forces due to tangential and radial accelerations are represented by $\mathbf{F_t}$ and $\mathbf{F_n}$ respectively. $\mathbf{T_{12}}$ is the inertial torque at the center of gravity of the link. Also, losses due to friction forces are assumed to be negligible and are not shown.

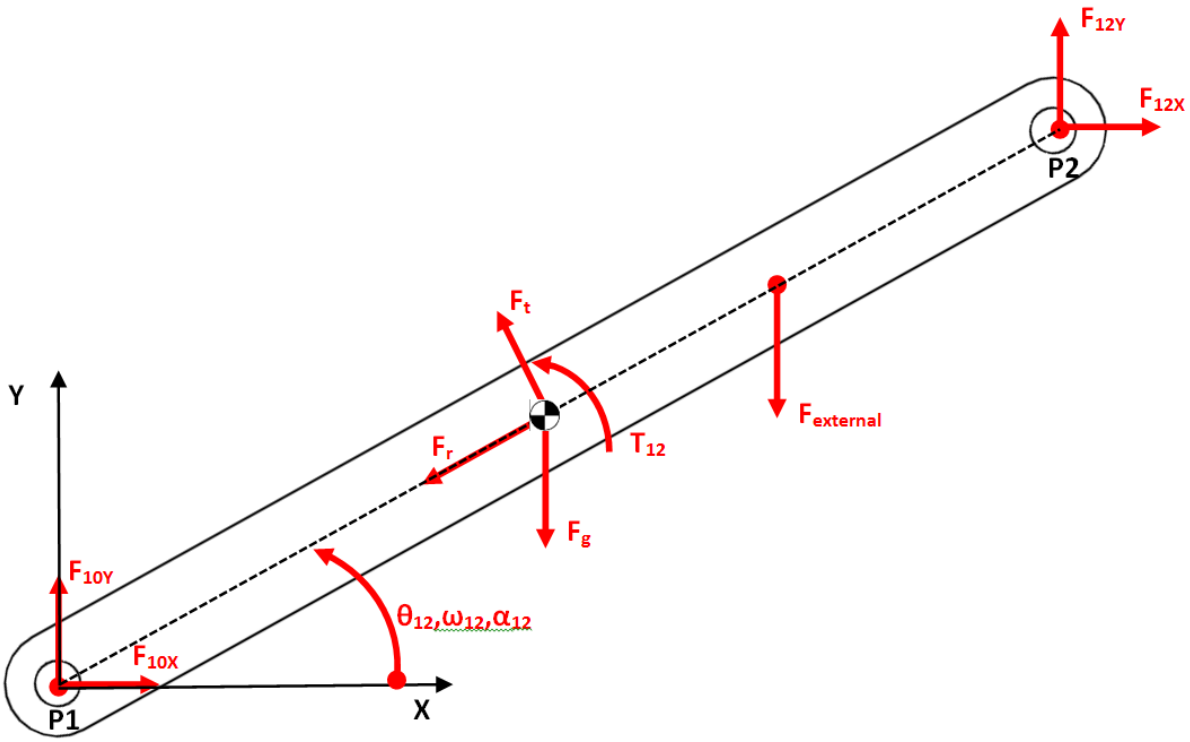

Figure 12: The forces for a generic link are shown, with an external force F.

The forces and moments for each link can be summed according to **equations (7)**, **(8)**, and **(9)**. In **equations (7)** and **(8)** the sum of forces in the x and y directions are summed and set equal to the x and y components of the radial and tangential forces, $\mathbf{F_t}$ and $\mathbf{F_r}$. The remaining forces at P_1 and P_2, along with $\mathbf{F_g}$ and $\mathbf{F_{external}}$ are summed on the left side of the equation. **Equation (10)** is the force of one link on another. From **Figure 12** this value is the force of link 1 on link 0, where the force on link 0 acting on link 1 would be the same magnitude but in the opposite direction.

$$\Sigma F_x = F_{t,x} + F_{r,x} = ma_{t,x} + ma_{r,x} \quad \textbf{(7)}$$

$$\Sigma F_y = F_{t,y} + F_{r,y} = ma_{t,y} + ma_{r,y} \quad \textbf{(8)}$$

$$\Sigma M_{CM} = I\alpha \quad \textbf{(9)}$$

$$F_{ab} = -F_{ba} \quad \textbf{(10)}$$

Free body diagrams can be drawn for each of the 4 links. While **equations (7)**, **(8)**, and **(9)** are used to solve the force equations for each link, **equation (10)** is used to equate the forces at the end of two connecting links. With the initial data, the system of equations is equal to the number of variables. The initial data consists of the links' weight, orientation, velocity, and acceleration. Also, in this way the effect of a known force and center of gravity to represent the container can be input into the system and analyzed. The result of solving the system of equations produces a unique solution.

3.1.2 Software simulation

A mathematical model was developed from the equations in the previous section. MATLAB was used to solve these equations, with given initial conditions. A simulation was used to calculate the fork and arm cylinder pressures for a full lift and lower cycle. A constant velocity, weight, and center of gravity were assumed. Throughout the simulation of an arm cycle, the fork cylinder was held at a constant angle, consistent with the experimental fork angle. Similarly, when the fork angle was varied in the simulation, the arm angle was held constant.

Simulations were run with similar conditions to the experimental tests. This included varying the center of gravity, weight, and velocity. Data points were recorded every degree across the range of the two cylinders. At each data point the system of equations was solved to determine arm and fork pressures, and then calculate cylinder force from these pressures. Selected theoretical results calculated from the simulation can be viewed in the results in section 4.3.

The relationship between the net cylinder force and the cylinder pressure is shown through **equation (11)**. Since the cylinder is a double acting hydraulic cylinder, the difference between the forces created by the rod and bore pressures is the net cylinder force. In the simulation, the back

pressure is assumed to be negligible, so P_{Bore} is zero during cylinder retraction and P_{Rod} is assumed to be zero during cylinder extension.

$$F_{cyl} = (P_{Bore} * A_{Bore}) - (P_{Rod} * (A_{Bore} - A_{Rod})) \quad \textbf{(11)}$$

3.2 Experimental setup

The experiment setup consisted of a McNeilus front loader refuse truck. The front loader linkage (

Figure 13) is consistent with the model shown in **Figure 8**. The larger cylinder is the arm cylinder, and the smaller cylinder is the fork cylinder. A container was fixed to the end of the forks. Cylinder pressure measurements were taken as the experimental weight was being lifted (arm cylinder retract) and also as the load was being lowered (arm cylinder extend). Inclinometer sensors were attached to measure the angle of the fork cylinders relative to the arms and the angle of the arm cylinders relative to the truck body. The truck body angle relative to the ground was negligible, for the test setup.

Figure 13: The test system is shown with both the arm and fork cylinders fully retracted and the two

inclinometer locations shown.

Both cylinders used are double acting cylinders as seen in **Figure 14**. During extend, fluid flows into the base end of the cylinder and displaces the fluid from the rod end. Similarly, during cylinder retraction the fluid flows from the rod end, displacing the fluid in the base end.

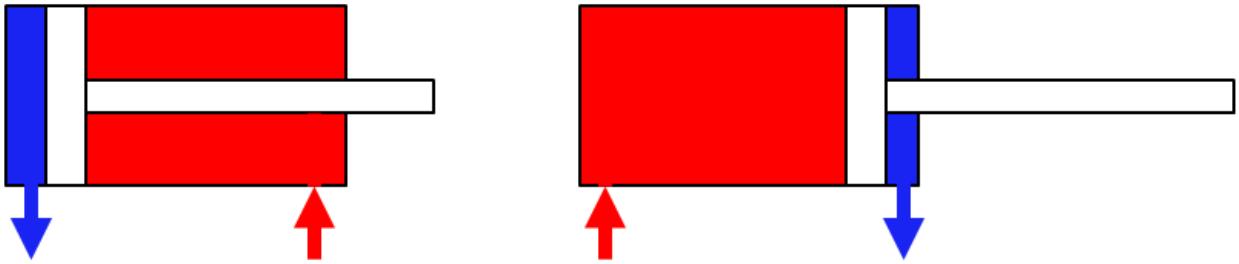

Figure 14: The left cylinder shows retraction, while the right cylinder shows extension. The red represents high pressure and the blue low pressure.

Pressure transducers are placed at the pump, arm cylinder ports, and fork cylinder ports. The cylinder ports were combined, so the input and output pressure of both is approximately the same. A sensor measures the pressure at both the inlet and outlet of the cylinders. When the base ends of the arm and fork cylinders are pressurized, the arms or forks are lowered. During cylinder retraction, the arms or forks are raised.

The force exerted by the rod of the cylinder is subtracted from the base end to determine the force at the ends of the cylinder shown in **equation (12)**. The effective rod area ($A_{rod,eff}$) is used to represent the difference between the cylinder bore and rod diameters that are used in **equation (11)**. Note that when the rod end is pressurized, the cylinder force will be in the opposite direction.

$$A_{base} * P_{base} - A_{rod,eff} * P_{rod} = F_{cyl} \quad \textbf{(12)}$$

The inclinometers use gravity as a reference to determine the orientation of the sensor. These were placed to measure the arm and fork cylinder angles as shown in **Figure 13**, or as shown in a close up view in **Figure 15**. The arm inclinometer is located at P_3 in **Figure 10**, measuring the angle at the arm pivot point. The fork inclinometer is located at P_6, and it is used to calculate the fork angle, which is the angle between the fork and the arm links. Since the sensors measure relative to gravity, to determine the fork angle, the arm angle is subtracted from the recorded fork angle. The output of the sensor varies linearly with the angle. By fully extending and retracting the cylinders, the maximum and minimum angles are determined. Since the sensors are linear, the in-between angles can be interpolated.

Figure 15: The fork angle sensor on the left and the arm angle sensor on the right were used to measure the angles of each cylinder.

Both the inclinometers and pressure sensors were connected to a HBM Somat electronic data acquisition system (DAQ), where the data was collected and stored and eventually analyzed in MATLAB. The transducers recorded at 1000 Hz in order to catch minor pressure spikes in the system, and the inclinometer position was recorded at 10Hz.

3.3 Testing procedures

Tests were performed with various known weights and locations, while the pressure and angles were recorded. The tests showed the effects of the weight and its location on the arm and fork pressures at different cylinder angles. These results are compared with the theoretical model.

A stationary test was performed to test the static forces during the arm raise and lowering. The test was performed with no weight, a medium weighted can, and a heavy weighted can. The container was in a fixed location on the forks. The linkage was moved thorough several specific positions, stopping at each position to obtain steady state values for the cylinder pressures. The fork and the arm cylinder angles were independently varied, so data could be collected for each.

Constant velocity tests were performed to determine the effects that weight and location had on the arm and fork pressures at different cylinder angles. The arms were raised and lowered with the different weights at a constant velocity. The fork angle was held constant at an angle of 75 degrees. A total of three different loads were compared (**Table 1**), while the velocity and center of gravity were held constant. This test was used to determine what effect the load has on the pressures of the arm and the fork cylinders.

Table 1: The external load placed on the forks ranged from 0 to 5050 pounds.

Varying Load cases	
Description	Value (lbs)
No load	0
Medium load - can plus 1 weight	3300
Heavy load - can plus 2 weights	5050

The velocity was varied to determine the subsequent effects on the arm and fork cylinder pressures. Several different velocities were compared (**Table 2**), ranging from 0 to 12.4 degrees

per second. Also, the linear velocity at the center of gravity at the container is shown as a reference.

Table 2: The angular speed of the arm link ranges from 0 to 12.4 degrees per second, and the container linear speed varies from 0 to 2.5 ft/s.

	Angular speed (deg/s)	Linear speed at container CG (ft/s)
Static	0	0
Low	3.5	0.7
Medium	7.4	1.5
High	12.4	2.5

With the medium weighted can, the location of the weight was varied to several locations as illustrated in **Figure 16**. The location for the center of gravity was varied forward, backward, and laterally. **Figure 17** shows the 4 different locations of the centers of gravity (CG) on the container. CG_1, CG_2, and CG_3 are located in a line 22.5", 29.8", and 36.9" respectively from the fork pivot. These three locations correspond to L_1, L_2, and L_3 in **Figure 16**. CG_4 is offset 23" to the side of CG_2. The three center of gravities that run down the center of the container produce different distances to the arm and fork pivots.

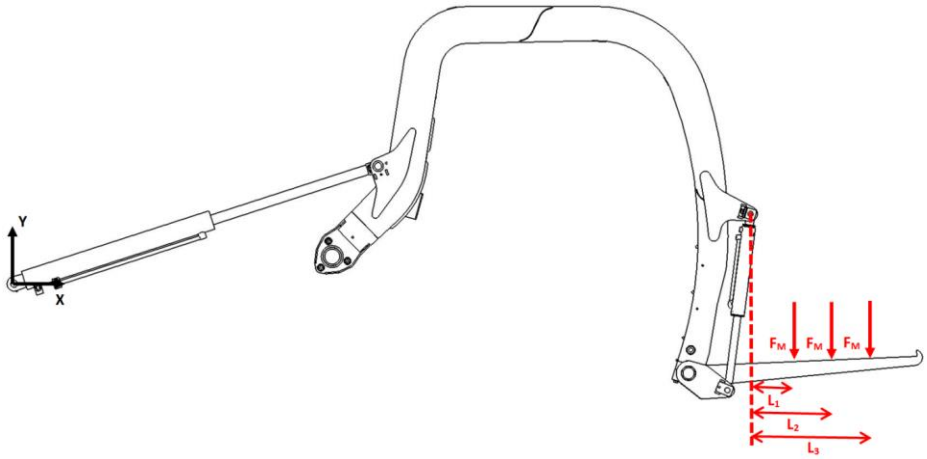

Figure 16: The varied CG for the weighted container can be seen at L1, L2, and L3

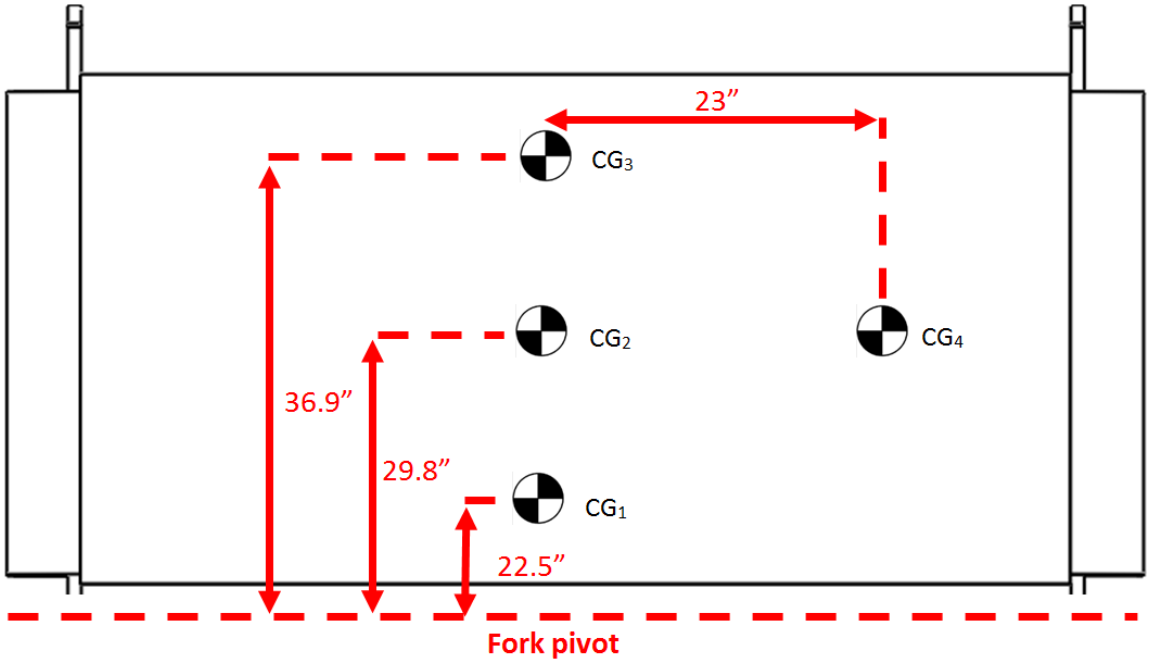

Figure 17: A top view of the container is shown, with CG_1, CG_2, and CG_3 running down the center of the container and CG_4 offset to one side of the container.

Table 3 is a descriptive summary of the 11 tests performed. Each one had data collected for both the arm and fork cylinders, although in many cases these would be expected to produce identical trends.

Table 3: The list shows the summary of conditions for each of the tests performed.

Test	Weight	Location	Velocity
Static	None	Center	None
Static	Medium	Center	None
Static	Heavy	Center	None
Constant	None	Center	Medium
Constant	Medium	Front	Medium
Constant	Medium	Back	Medium
Constant	Medium	Center	Low
Constant	Medium	Center	Medium
Constant	Medium	Center	High
Constant	Medium	Right	Medium
Constant	Heavy	Center	Medium

A MATLAB simulation was used to vary the cylinder angles in the theoretical model so the data could be plotted against empirical data for various weights and locations. The values for the weights and locations of the links were determined from the physical components. The weight and center of gravity of the container and weight inside were measured, and these values are used for the theoretical model.

CHAPTER 4: RESULTS

The methods previously described in Chapter 3 were used for the data collection. Results from both the theoretical model and experimental data gathering will be presented. Results from the static scenario are first examined. Various loads were examined for comparison. Next, the constant velocity results are examined using different loads, locations (center of gravity), and speeds.

Various graphs are presented that show either the arm or fork data, or in some cases both. The data is shown as the net force at the pin of each cylinder. While the raw data collected is pressure at each end of the cylinder, the pressures are used to calculate the force at each end. Then the forces are subtracted to calculate the net force on the cylinder.

4.1 Static load

Static loads are compared at both the arm and fork cylinders. The arm and fork cylinders were extended or retracted for a short distance, then stopped for several seconds to ensure that the cylinder pressure had achieved steady state.

Figure 18 shows the forces at the arm cylinders, with the fork angles held a constant angle. Negative forces indicate the force is acting in the opposite direction. As the arm cylinders fully retract, the center of gravity of the arms is shifted backwards and the force is exerted in the opposite direction. Three load conditions are shown: no weight, medium weight, and heavy weight. The no load condition shows the forces at the cylinders due to the links in the system. The medium weight includes the container and an additional weight, which together weigh 3,300 pounds. The heavy weight includes additional weights that are symmetrically spaced for a total of 5,050 pounds. The force as measured as the cylinder was retracted.

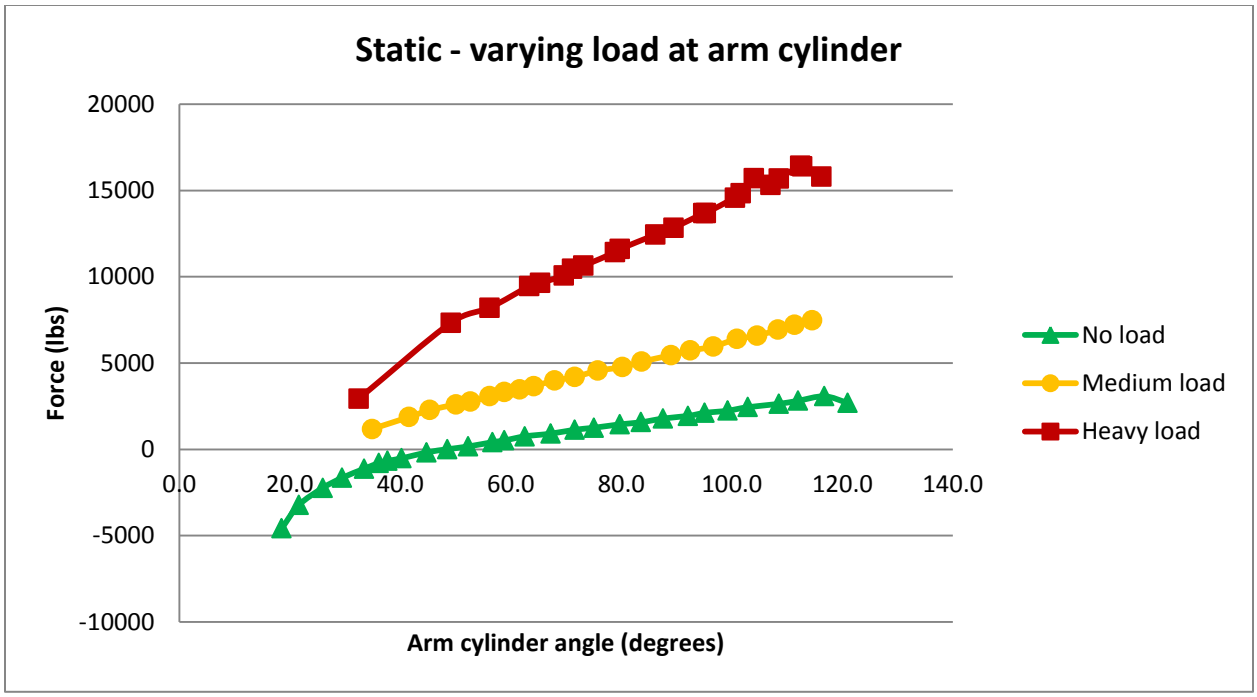

Figure 18: The force results of the arm cylinder were measured for no load (0 pound), medium load (3,300 pounds), and heavy load (5050 pounds).

Figure 19 shows the forces of the fork cylinders, while the arm cylinders were held at a constant angle. Two loads are shown: no weight and medium external weight. For no load, there is little change in the force at the cylinders, with a range of approximately 450 pounds, while the medium load case has a much higher range of values.

Figure 20 shows an up and down arm cycle, with a no load condition and a constant fork angle. The pressure was measured in static state first during cylinder retract, or arm raise, and then during the cylinder extend, or arm lower. The retract force is about 250 pounds higher than the extend force for most points; however, it extends to as much as 400 pounds higher to as low as 100 pounds higher during retract.

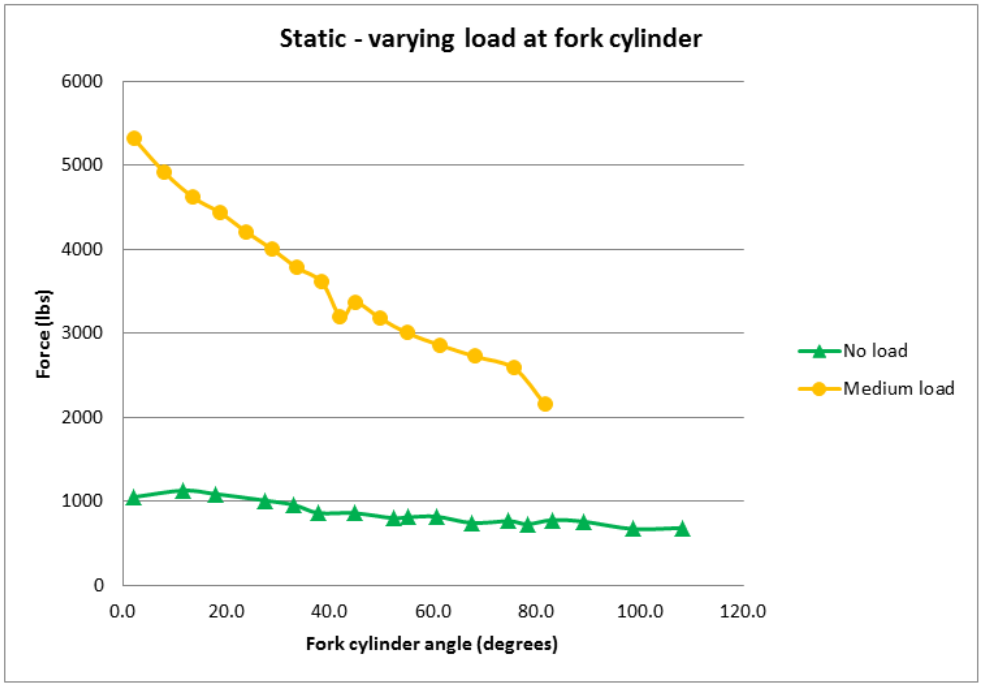

Figure 19: The force results of the fork cylinder were measured during no load and medium load (3,300 pounds) conditions.

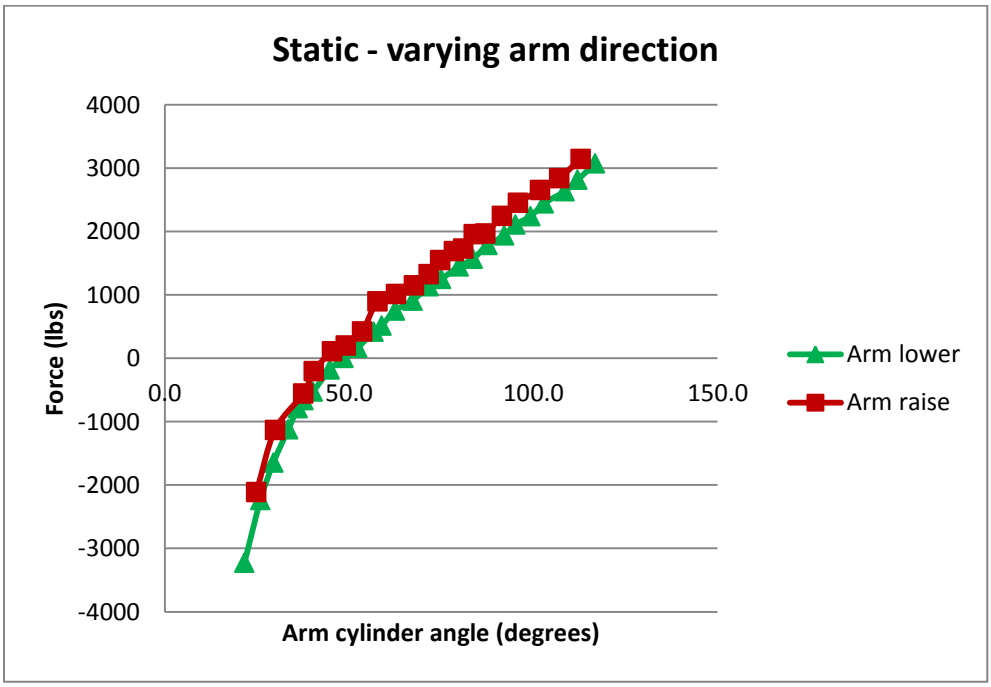

Figure 20: The force results of the arm cylinder were measured at a static position and no addition weight, during arm raise and lower.

4.2 Constant velocity

The effect of constant velocity motion on the arm and the forks was tested. Several variables were tested including load, velocity, and center of gravity. The effect that these had on the arm and fork cylinders was examined through the testing.

When comparing each variable, the other two are held constant. For the constant load scenarios, a medium weight of 3,300 pound was used. With a fixed velocity, the radial velocity was kept around 7.5 deg/sec. The standard location for the center of gravity is spaced equidistance between the two forks and halfway back from the front of the container, which is about 24" back from the front. The standard center of gravity can also be seen as point 2 in **Figure 17**.

First, a test was conducted with a constant load, fixed velocity and standard center of gravity. The experimental data for constant velocity was compared in **Figure 21.** Experimental data from both cylinder extend and retract are shown. Similar to the static results, the cylinder extension and retraction produced different results. During arm raise, the difference between the arm raise force and arm lower force was at its minimum of about 250 pounds at 30 degrees, while this difference was nearly 700 pounds at an angle of 100 degrees.

For the heavy loads, the data exhibited significant variation due to the dynamic characteristics of the linkage itself, which made the actual pressure values difficult to record. A moving average filter was used to remove some of the variation in the constant velocity case, with medium and heavy weight loads. It was used to average 500 data points, or .5 seconds, for heavy loads and 250 data points, or .25 seconds, for the medium loads. **Figure 22** shows the initial pressure data recorded from the arm cylinder and the data after the filter has been applied. The filter was used in the data analysis for heavy weight loads and medium weight loads as the

variation does not have a significant effect on the lower weight loads. Note that the moving average causes a slight delay in the data trends, which can be as high as .5 second offset.

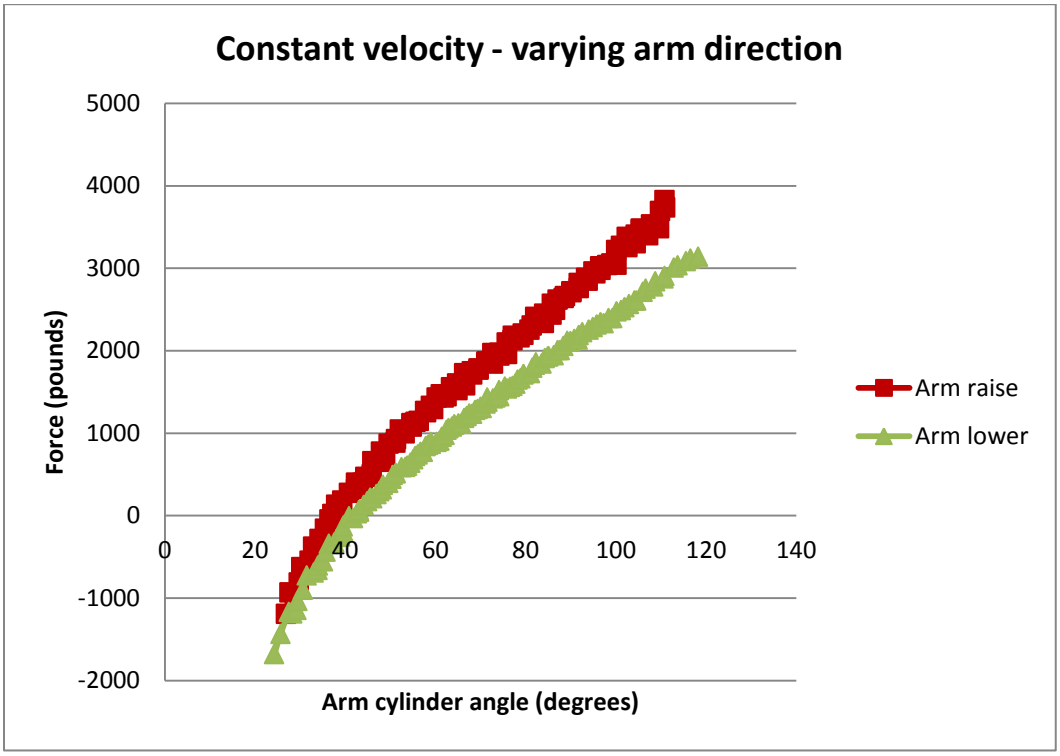

Figure 21: The force results of the arm cylinder were measured at constant velocity and no additional weight, during arm raise and lower.

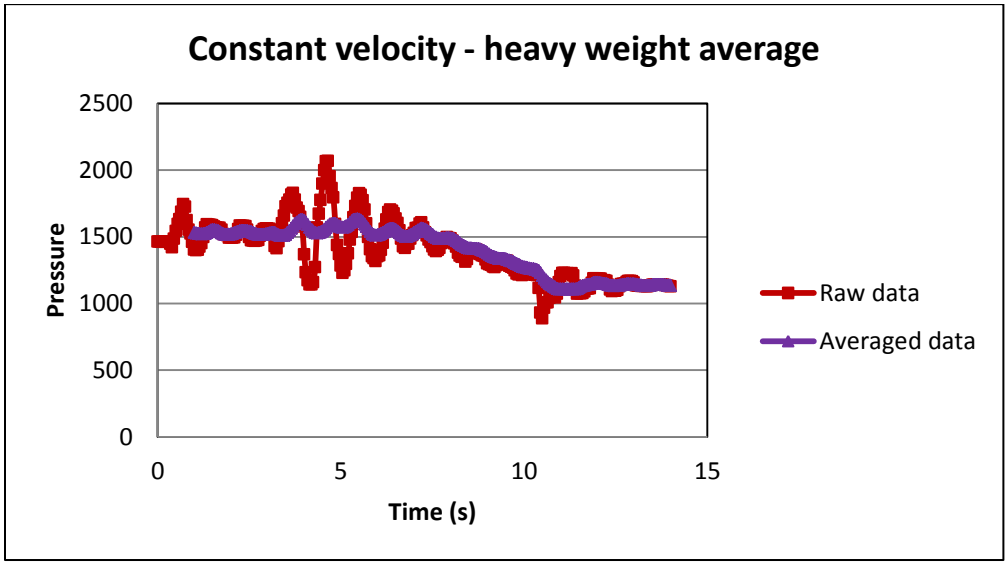

Figure 22: A moving average is overlaid on top of the raw data collected.

In the static case the system was allowed to achieve steady state, so the variation did not affect the results. However, for constant velocity cases, the variation could not be ignored. For the remaining sections the moving average is used to filter the data points that use the medium and high loads, before the values are displayed on graphs.

4.2.1 Varying load

Figure 23 shows a constant velocity scenario, with three different external loads. The graph shows the constant velocity portion of the can, during the arm raise. The net force on the ends of the cylinder is shown compared to the angle of the arm cylinders. The arms are moving at an angular speed of about 7.5 degrees per seconds, or about 1.5 ft/sec at the center of gravity of the weighted container.

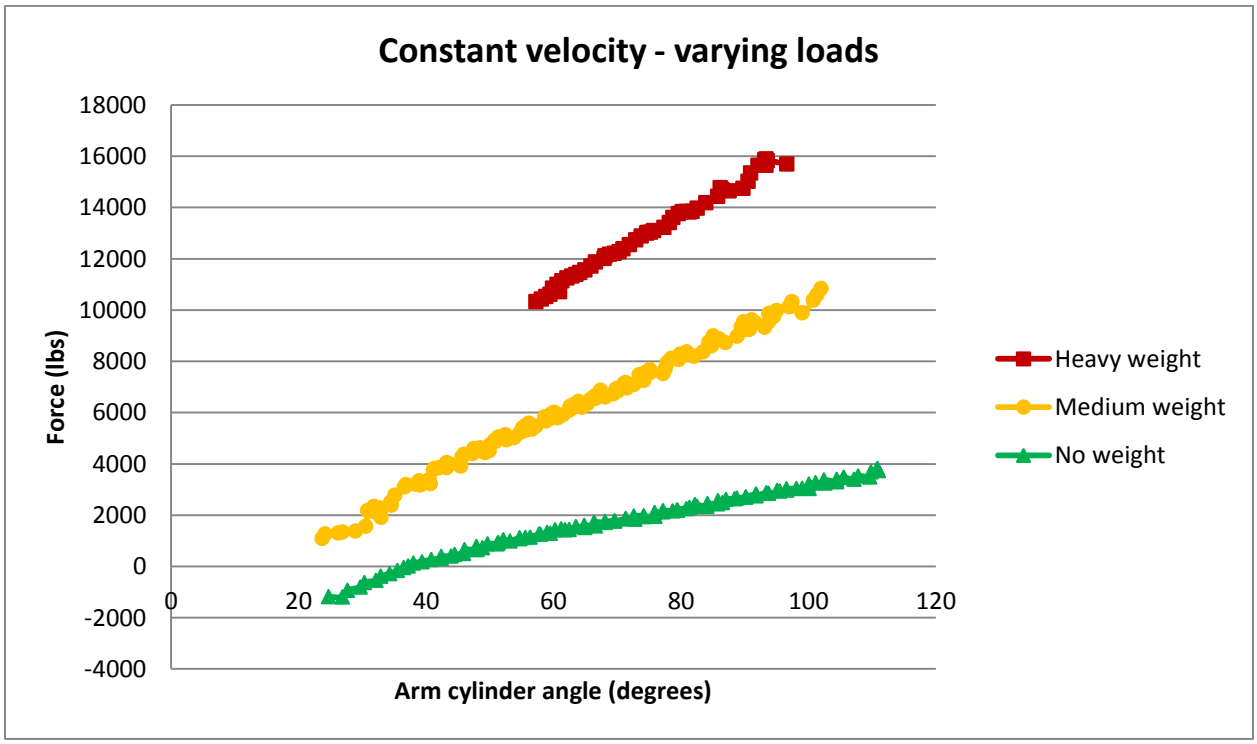

Figure 23: The force results of the arm cylinder were measured at constant velocity for three different loads: heavy (5,050 pounds), medium (3,300 pounds), and no load (0 pounds).

4.2.2 Varying velocity

The graphs in this section compare the arm cylinder angles versus the force exerted by the cylinder at varying velocities. These tests used a medium weight (3,300 pounds) and lifted it at a low speed, medium speed and high speed. **Figure 24** shows the force of the arm cylinder, relative to the arm cylinder angle, at various speeds.

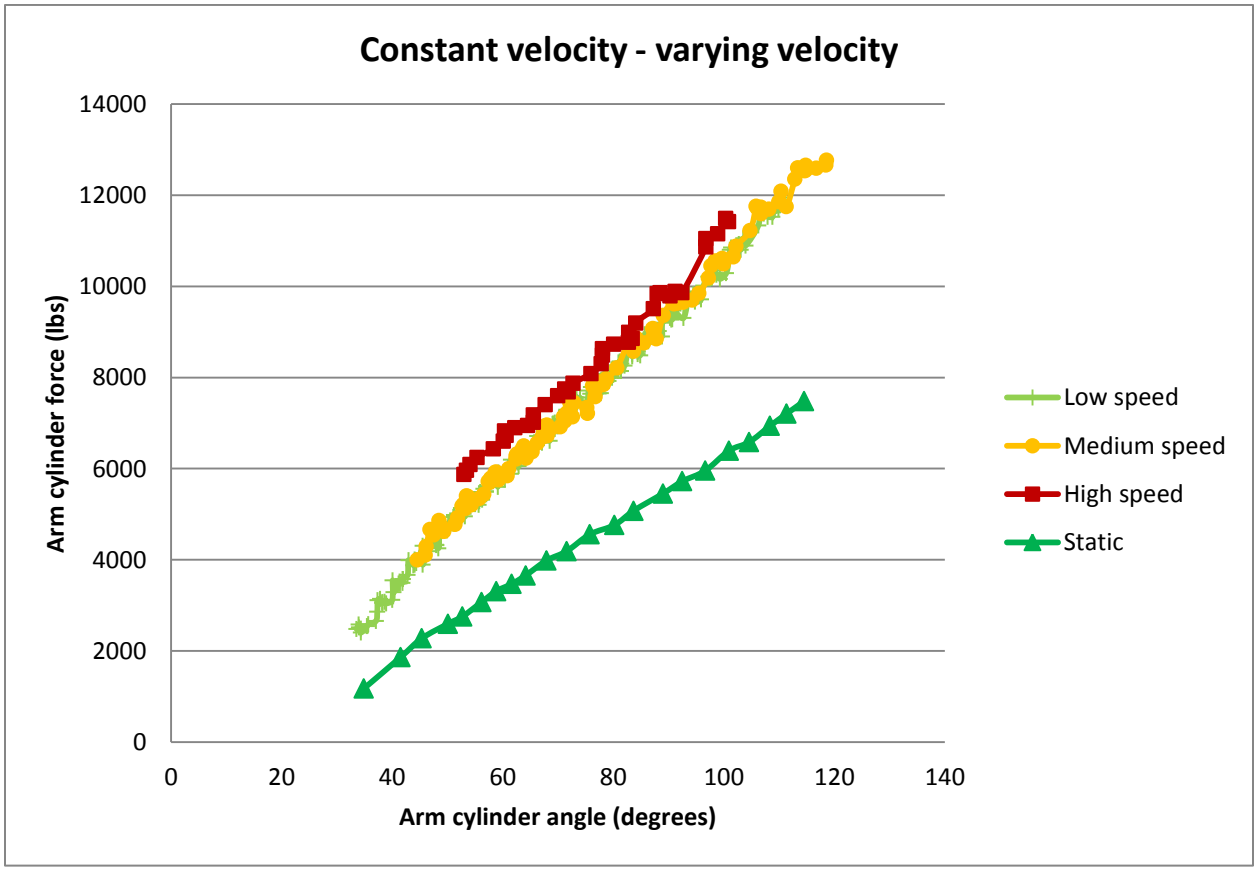

Figure 24: The force results of the arm cylinder were measured at four different arm speeds, which were stopped (0 deg/s), low (3.5 deg/s), medium (7.4 deg/s), and high (12.4 deg/s) speeds.

The non-zero velocities range from .7 ft/s to 2.5 ft/s; however, there is little difference in arm force between the three speeds. The arm force at the medium speed was about 75 pounds higher than the low speed, while the high speed was about 250 pounds higher than the low speed.

All three velocities had higher arm forces than the static forces, ranging from 1500 pounds at 40 degrees to over 5000 pounds of force at the arm cylinder angle of 115 degrees.

4.2.3 Varying center of gravity

The effect of varying the location of the center of gravity along the centerline of the container can be seen in **Figure 25**.

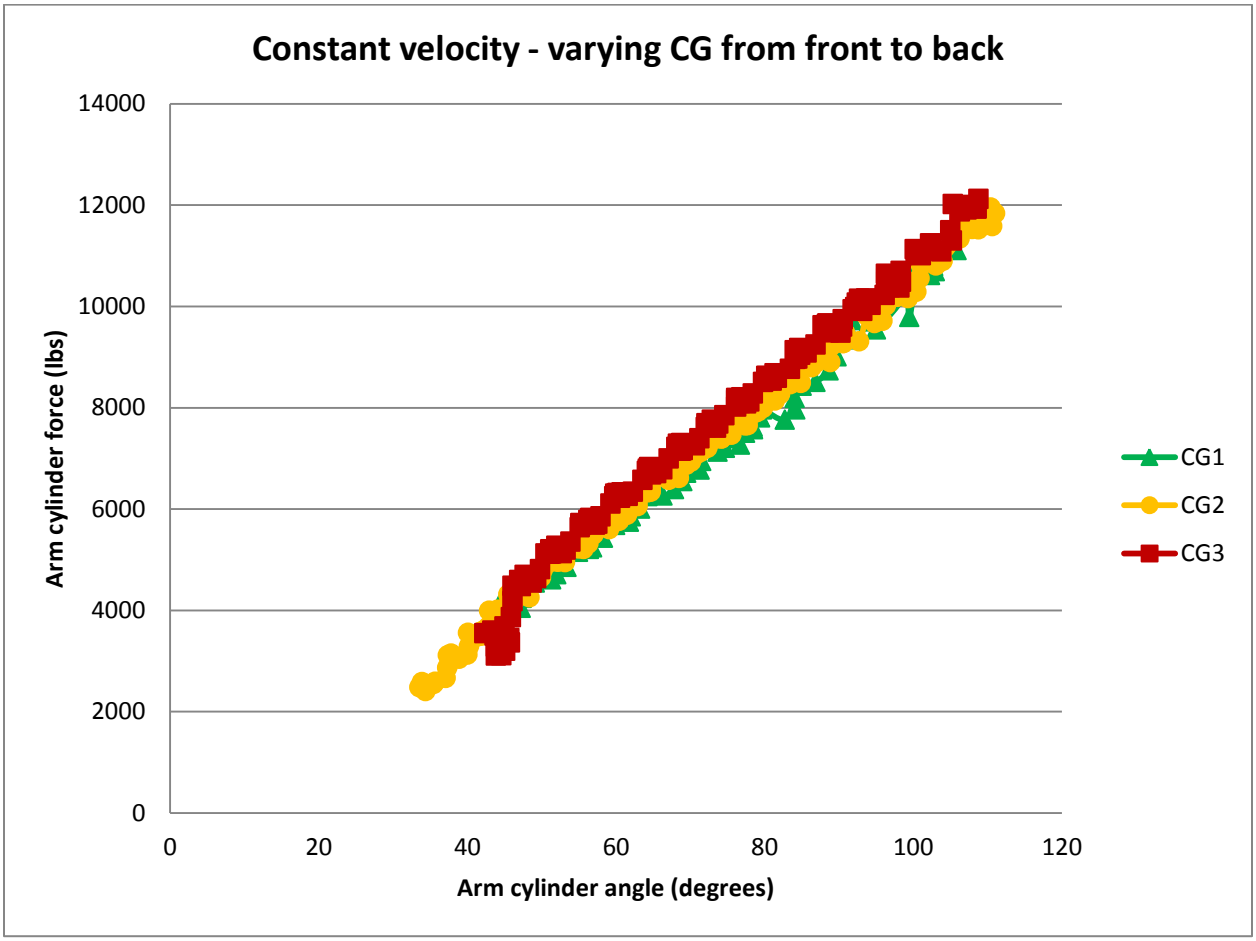

Figure 25: The force results of the arm cylinder were measured at medium weight (3,300 pounds), for the three different front to back CG locations.

The center of gravity location slightly increased the force on the arm cylinder. CG_2 had about 200 pounds more force on average than CG_1, and CG_3 had about 600 pounds higher force at the cylinder than CG_1.

Figure 26 compares CG_2 and CG_4, where CG_4 is offset to one side. Since the arms are symmetric from side to side, CG_4 can be placed on either side of the can center and still produce similar effects. Varying the center of gravity to one side had a minimal effect on the arm force. The off-center CG_4 averaged 100-200 pounds higher than the center of gravity that was in the center.

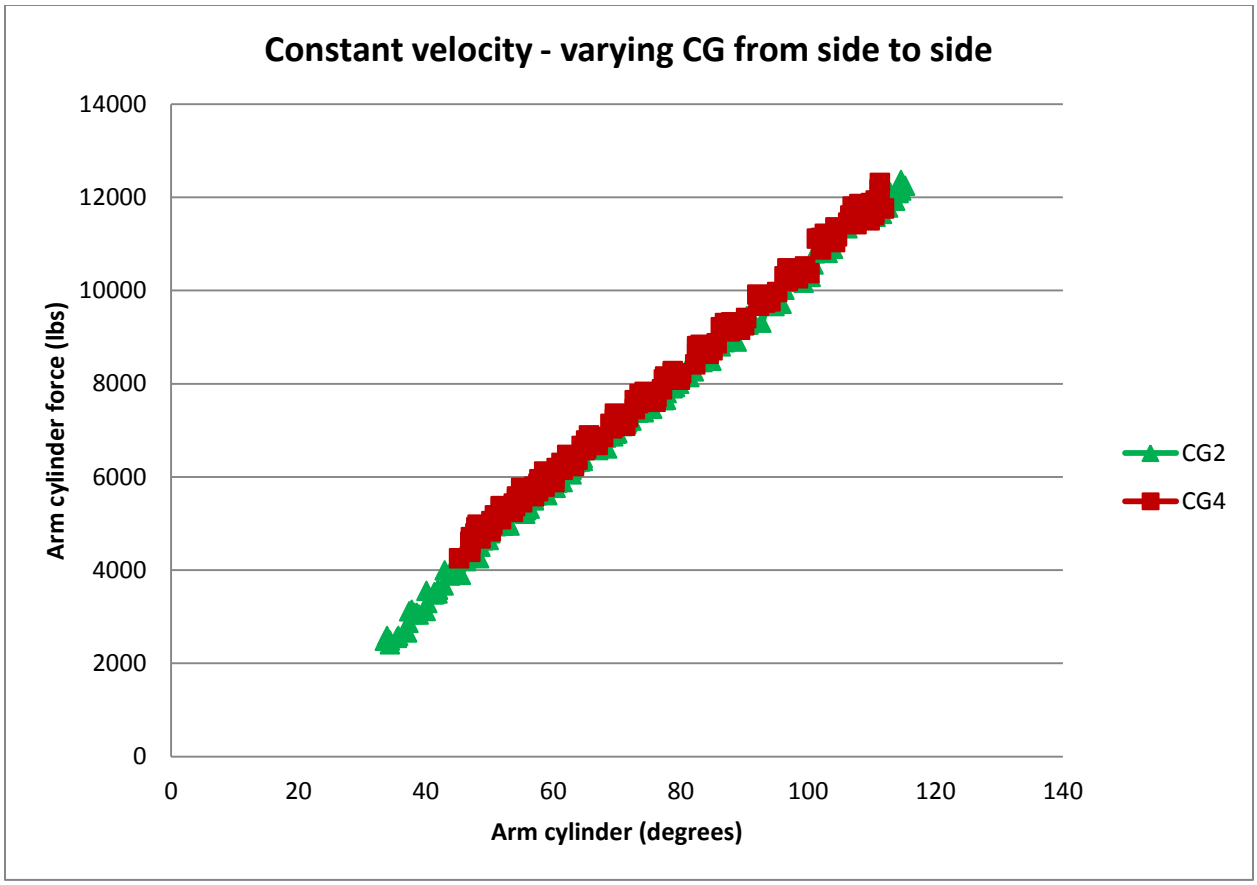

Figure 26: The force results of the arm cylinder were measured at medium weight (3,300 pounds) for the two lateral CG locations.

4.3 Combined theoretical and experimental results

The experimental results from section 4.2 will be compared to theoretical results produced by the simulation, using a medium loaded container (3,300 pounds). Results from cylinder retract and extend are shown compared to the theoretical results, for both static

conditions and a constant velocity tests. The center of gravity was assumed to be in position CG_1 in **Figure 24**.

The theoretical model and the experimental data for a static medium load are compared in **Figure 27**. The theoretical results are lower than the experimental data gathered, during both the arm retract and extend. In the experimental data the forces during arm extend are higher than the forces during arm retract. From cylinder angles of 50 to 100 degrees the theoretical results match the curves of the experimental data. In this range the experimental data from arm retract is about 200-400 pounds higher than the theoretical model; however, outside this range the difference between the curves is larger.

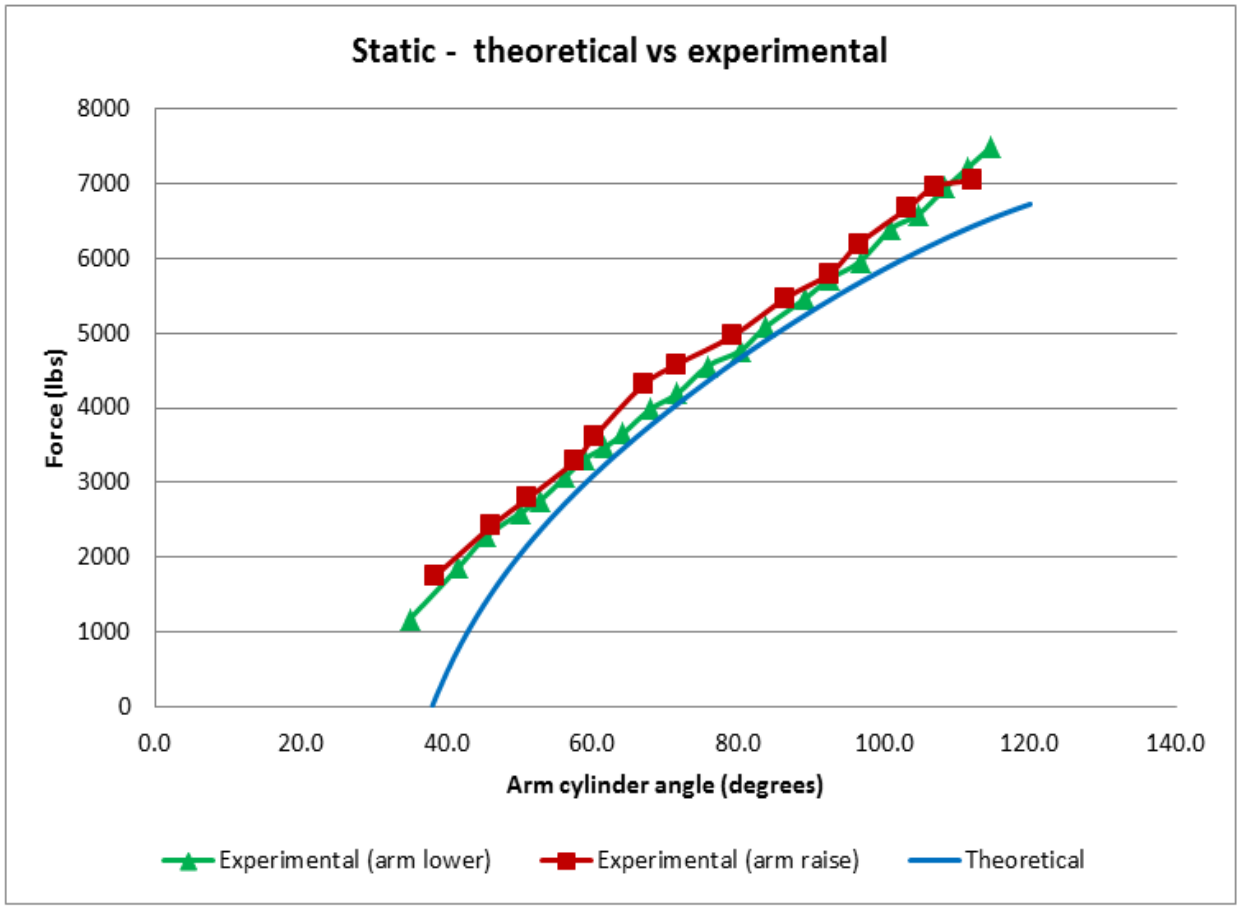

Figure 27: The experimental force was measured at the arm cylinder and compared to the theoretical results.

For a constant velocity of 9.2 deg/s, the medium load was used again to compare the experimental results to the theoretical results. The forces produced in the arm cylinder are shown in **Figure 28**. The graph shows that the force when the arms move up is higher than the force during the arms down. When the arm cylinder angle is between 50 and 100 degree, the theoretical results are around 200-400 pounds lower than the experimental results. Outside of this range, the difference increases. During this range the forces at the arm cylinder during arm raise is about 1,000-1,500 pounds higher than during cylinder lower.

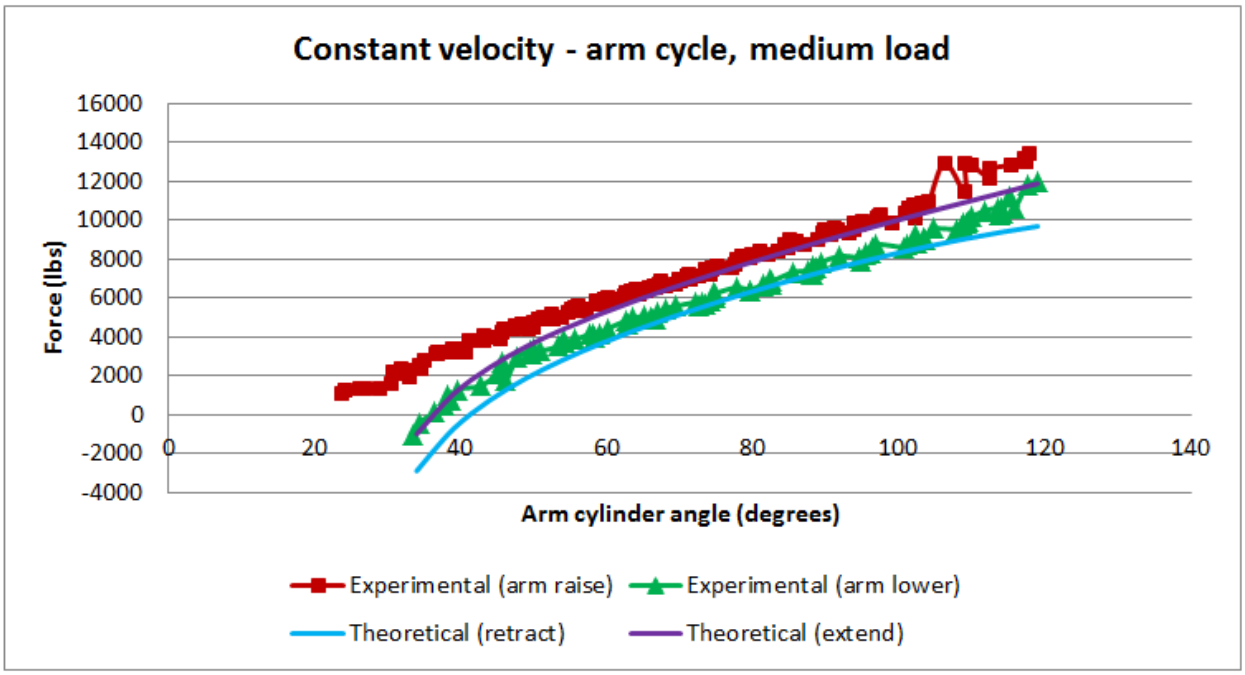

Figure 28: The experimental force data was measured at the arm cylinders in constant motion and compared to the theoretical results, during arm raise and lower.

4.4 Experimental error

The weight error due to the arm cylinders is shown in this section, while the fork cylinders are held constant. The experimental arm cylinder pressures and link angles are used to estimate the weight on the fork. The expected weight is calculated from the experimental data

and is subtracted from the actual weight to determine the error. **Figure 29** shows the forces involved in estimating the expected force.

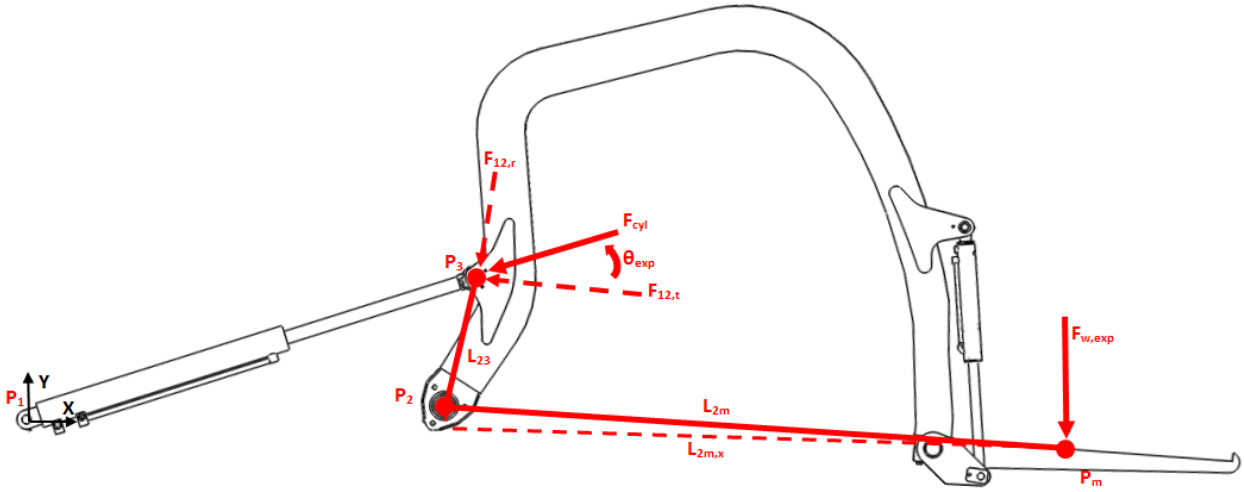

Figure 29: The mechanical advantage of the cylinder and external load are shown relative to the pivot point P2.

The arm cylinder force, $\mathbf{F_{cyl}}$, can be broken up into the perpendicular force, $\mathbf{F_{12,t}}$, and parallel force, $\mathbf{F_{12,r}}$. These force components of the arm cylinder are tangential and radial relative to the link L_{23}. The distance between the arm and fork pivot is a fixed length L_{23} that rotates about P_2. The arm cylinder and length L_{23} are offset from perpendicular by an angle, $\boldsymbol{\theta_{exp}}$. **Equation 13** expresses $\boldsymbol{\theta_{exp}}$ as a function of the angles of the vectors from **Figure 10**.

$$\theta_{exp} = \theta_1 + \theta_2 - 90 \quad \textbf{(13)}$$

The force of the expected weight, $\mathbf{F_{w,exp}}$, on the fork is located at the CG of the container. This force is located at a lateral distance, $L_{2m,x}$, away from the fork pivot, P_2. The distance $L_{2m,x}$ is shown in **equation (14)** as a combination of the vector x-components from **Figure 10**.

$$L_{2m,x} = R_{23,x} + R_{34,x} + R_{46,x} + R_{6m,x} \quad \textbf{(14)}$$

The mechanical advantage at P_2 from $\mathbf{F_{cyl}}$ is equal to the mechanical advantage of $\mathbf{F_{w,exp}}$ at P_2. **Equation (15)** shows this comparison, where $\mathbf{F_{cyl}}$ and $\boldsymbol{\theta_{exp}}$ are calculated from the experimental pressure and angles. Note that $\mathbf{F_{cyl}}$ is doubled to account for both cylinders.

$$2 * F_{cyl} * \cos\theta_{exp} * L_{23} = F_{w,exp} * L_{2m,x} \quad \textbf{(15)}$$

From **equation (15)** the force of the expected load, $\mathbf{F_{w,exp}}$, is calculated. To determine the weight error, $\mathbf{e_{weight}}$, the force $\mathbf{F_{w,exp}}$ is subtracted from the actual weight, $\mathbf{F_{w,real}}$, as shown in **Equation (16)**. A negative error means that the experimental predicted weight is lower than the real load, $\mathbf{F_{w,\,real}}$.

$$e_{weight} = F_{w,exp} - F_{w,real} \quad \textbf{(16)}$$

For the three weight error graphs, the fork angle is held at a constant angle of 75 degrees between the fork and arm. For weight error due to varying loads, the data from **Figure** 23 was analyzed. This was the load varying case at constant velocity. **Figure 30** compares the error from these three different load cases. The error was within about 500-700 pounds for the heavy weight load case scenario, and within about 300 pounds or less for the medium weight load case scenario. This is an error of 10-15%.

The weight error from data gathered in the varying velocity at medium load from **Figure 24** was compared.

Figure 31 shows the error from the velocities. The medium and low speed has similar errors within 400 pounds, with a higher error at a higher angle. The high speed had an error of about 300-500 pounds.

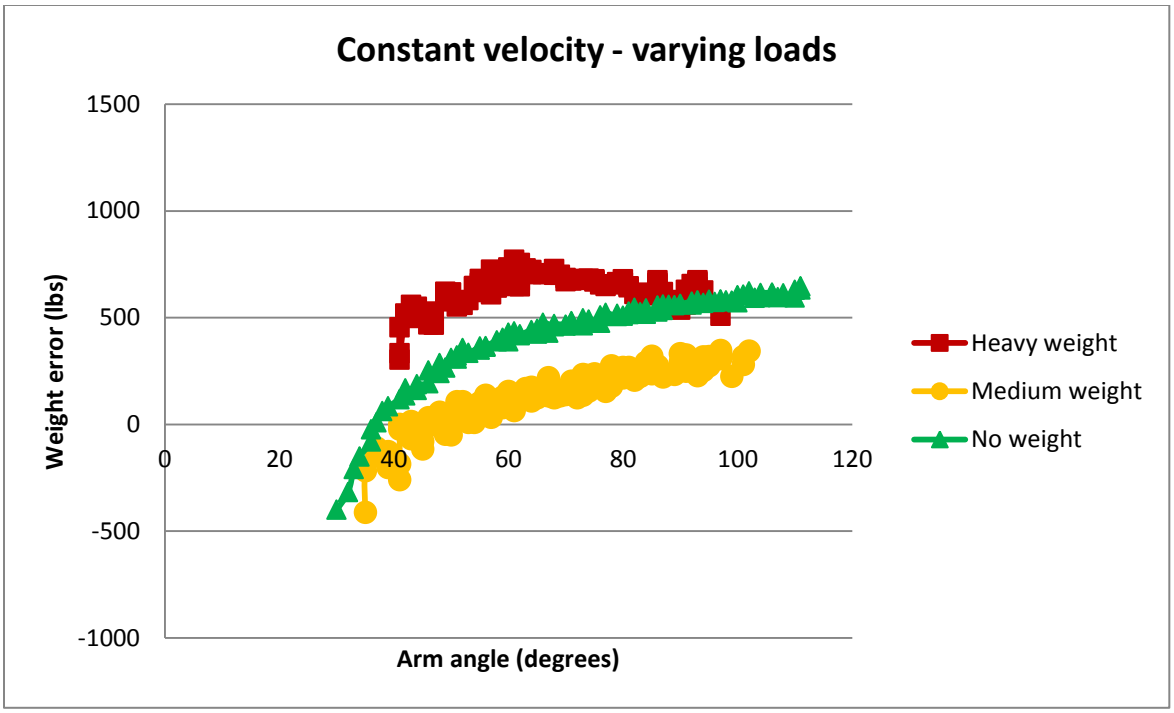

Figure 30: The error between the theoretical and experiment load was compared, for the varying load data.

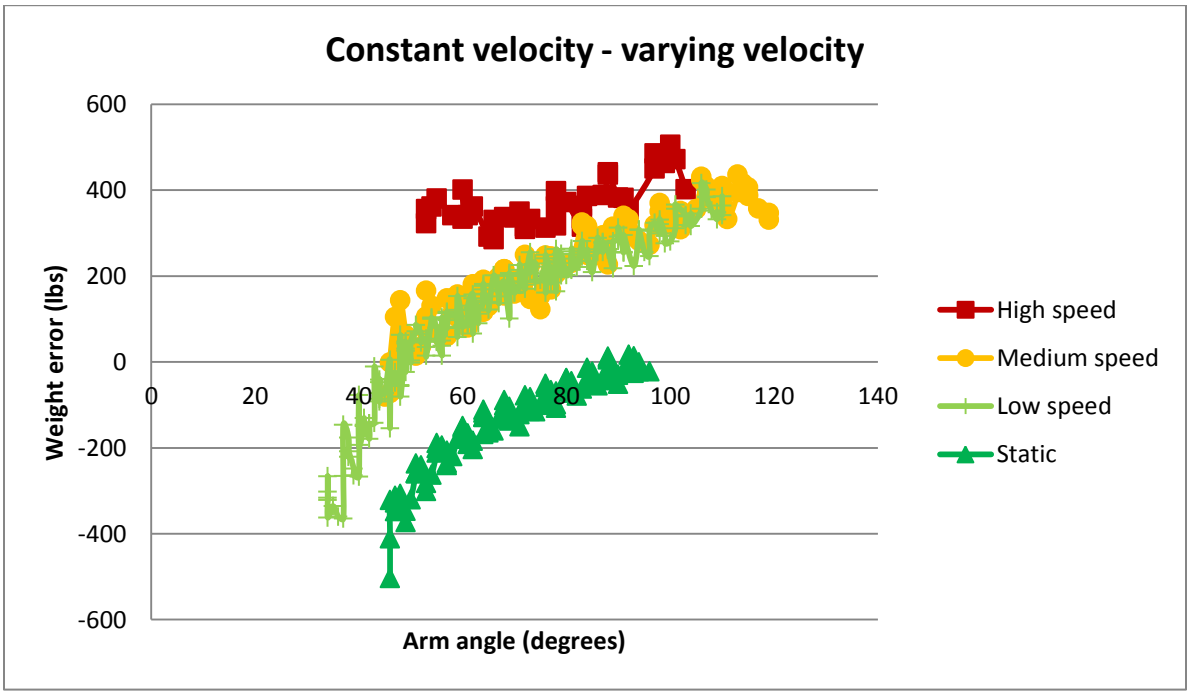

Figure 31: The error between the theoretical and experiment load was compared, for varying velocity.

The center of gravity from **Figure 25** was evaluated to determine the error. **Figure 32** shows the error for the medium load varying CG. All 3 graphs have nearly identical errors between 50 and 100 degrees. At 50 degrees the error is approximately 500 pounds below the actual weight and at 100 degrees the error is about 50 pounds above the actual weight.

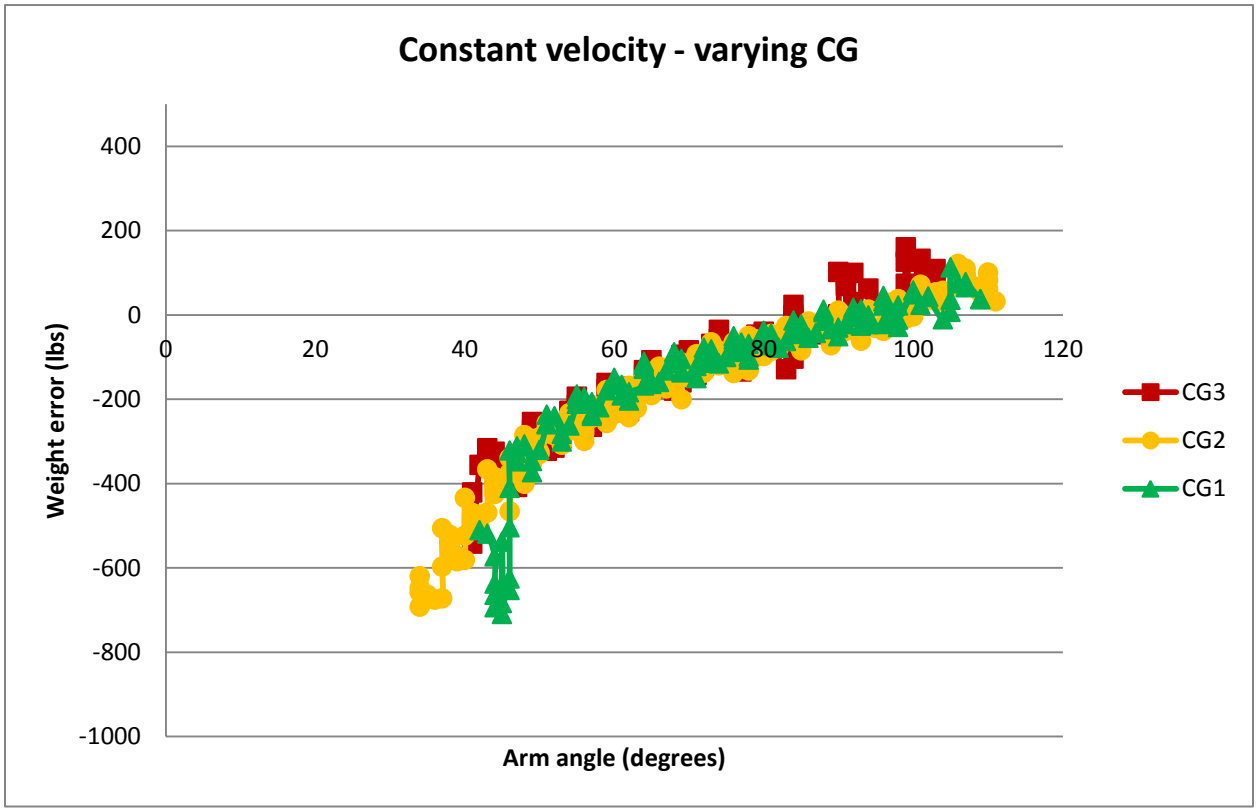

Figure 32: The error between the theoretical and experiment load was compared, for varying center of gravity.

CHAPTER 5: DISCUSSION AND CONCLUSIONS

Weight measurement has been around for many years; however, as technology continues to advance, additional tools and techniques are being developed. While, many of the same principles of the original weight measurement systems are still used, the accuracy is much greater. Higher accuracy in measurement sensors allows new systems to be developed that use these tools in new ways.

As weight becomes more important in many industries, keeping track of how much a system or payload weighs becomes increasingly critical. The need for accurate information is apparent in the transportation industry, where there are many regulations for traveling on roads. A number of systems have been introduced in order to resolve the issue of on-board weight measurement; however, these systems often have a high cost or weight associated with them. Both of these are undesirable traits. By measuring the cylinder pressures and angles during various tests and using these to determine the force, the weight of a container being picked up can be estimated. Furthermore, the weight of a payload can be estimated by measuring the weight of a full container as it is raised and the empty container as it is lowered, which simulates a dumped payload. The change in weight between the raise and lower motions can be used to calculate the payload weight that is dumped from the container.

The purpose of the testing was to determine the main factors of the external weighted container that could affect the force at the cylinders. The three tested factors varied weight, velocity, and center of gravity. Varying weight was tested in both a static state and a constant velocity state. While the velocity was held constant, tests were run with different constant velocities. Finally, the center of gravity was shifted both further out and laterally to determine the effects.

There are several potential error sources in the data. The hydraulic oil temperature heated up throughout the testing, which can decrease the viscosity and cause less resistance in the fluid. Another source of error is introduced with heavier weights. For larger weights, as the arm moved a dampened oscillating motion occurred. In order to account for the motion, a moving average filter was introduced to average the data, which could affect the integrity of the data. Also, side load forces, environmental differences, and friction losses were not measured.

From the variable load testing results, the data showed that the force at the cylinder was affected by the weight of the load. During both the static testing and the constant velocity testing, the force increased and remained near linear with respect to the cylinder force. When comparing the cylinder retract and extend forces, there was a difference. One of the main contributing reasons to this may be hysteresis in the cylinders.

When testing over various constant velocities, there was a little change in cylinder forces between the low to high velocities. Again, much of the curve was linear, once the system reached a constant velocity condition. Varying of the center of gravity impacted the force curves. While the slope of the graph appeared similar, the increase in distance from the pivot offset the forces on the graph. Likewise, moving the center of gravity to one side increased the force of the cylinder as well, although only slightly compared to the other factors. The additional force may be due to a higher load being induced on one of the two cylinders. Since both cylinders are connected at the inlet, an increase in pressure required to move one cylinder would increase in pressure and force in both cylinders.

The error due to weight, velocity, and center of gravity was compared. The error due to varying weight was within about 300 pounds for the medium load and 700 pounds for the heavy load. This is up to 10-15% error. In the error calculations the weight of the links was

neglected, which could be a cause for some of the error. Neglecting link weights would cause the error to be higher than expected at larger angles, which could contribute to the error not remaining constant compared to angle. The error between the different velocities was smaller but still significant at around 100-200 pounds between the low and high speeds. When varying the center of gravity, for the majority of the angles there was no discernable difference between the errors.

The errors in the varying weight graph varied with angle. This same result can be seen throughout all the error graphs. This shows that there are additional forces that need to be investigated. The error results for the medium and heavy weight were around 10-15%, but the results still requires further investigation into the sources for the error. Future testing will need to be performed to investigate friction forces in the cylinder and at the pivot points. Additionally, losses due to side loads and particular environmental conditions may need to be evaluated. Combined, all of these factors may be the main contributors to the error.

Continuing research could investigate the sensitivity that each of the variables has on pressure. Future testing could be used to evaluate additional factors that affect the lifting motion, such as environmental conditions, cylinder side forces, hysteresis, and friction losses. Additionally, testing the effects of weight, velocity, and center of gravity on a different linkage system could be used to further validate the theory.

BIBLIOGRAPHY

[1] T. Ono, K. Kameoka, and K. Nakajima, "Studies on Dynamic Measurement Method of Mass and Weight (Part 1)," *JSME*, vol. 22, no. 166.

[2] R. L. Hannah and S. E. Reed, *Strain Gage Users' Handbook*. London, UK: Chapman and Hall, 1992.

[3] U. E. P. Agency, "Municipal Solid Waste Generation, Recycling, and Disposal in the United States: Facts and Figures for 2012," 2012.

[4] F. H. A. US Department of Transportation, "Federal-Aid Policy Guide," *FHWA*, 2010. [Online]. Available: http://www.fhwa.dot.gov/legsregs/directives/fapgtoc.htm.

[5] J. L. Meriam and L. G. Kraige, *Engineering Mechanics Volume 2*, 6th ed. Hoboken, NJ: John Wiley & Sons, Inc, 2010.

[6] T. I. B. of W. and Measures, "The International System of Units (SI) 8th edition," 2006.

[7] H. R. Jenemann and E. Robens, "Indicator system and suspension of the old egyptian scales," *Thermochim. Acta*, vol. 152, no. 1, pp. 249–258, Oct. 1989.

[8] "The History of Weighing," *Avery Berkel*, 2009. [Online]. Available: http://www.averyberkel.com. [Accessed: 03-Jun-2015].

[9] E. Hartig and T. Weiss, *Iconographic Encyclopedia of the Arts and Sciences: Applied Mechanics*. Philadelphia: Iconographic Publishing Co., 1890.

[10] R. M. O'Grady, Z. Pobocha, T. Rapa, F. Holken, and J. A. Giron, "Triple-beam balance," U.S. Patent: D568190, issued date May 6, 2008.

[11] R. A. Kopp. "Scale beam." U.S. Patent: 1872465, issued date 16-Aug-1932.

[12] B. G. Liptak, Ed., *Instrument Engineers' Handbook: Process Measurement and Analysis*, 4th ed. Boca Raton, FL: CRC Press; ISA Press, 2003.

[13] "Spring Balance," *Encyclopedia Britannica Online*. Encyclopedia Britannica, 2015. [Online]. Available: http://www.britannica.com/technology/spring-balance. [Accessed: 03-Jun-2015].

[14] V. Button, *Principles of Measurement and Transduction of Biomedical Variables*. London, UK: Elsevier Science, 2015.

[15] F. Abe, H. Akimoto, et al, "Measurement of the Top Quark Mass with the Collider Detector at Fermilab," *Phys. Rev. Lett.*, vol. 82, no. 2, pp. 271–276, Jan. 1999.

[16] S. Dürr, Z. Fodor, J. Frison, C. Hoelbling, R. Hoffmann, S. D. Katz, S. Krieg, T. Kurth, L. Lellouch, T. Lippert, K. K. Szabo, and G. Vulvert, "Ab initio determination of light hadron masses.," *Science*, vol. 322, no. 5905, pp. 1224–7, Nov. 2008.

[17] M. Mayor and D. Queloz, "A Jupiter-mass companion to a solar-type star," *Nature*, vol. 378, no. 6555, pp. 355–359, Nov. 1995.

[18] "Strain gauge," *Encyclopedia Britannica Online*. Encyclopedia Britannica, 2015. [Online]. Available: http://www.britannica.com/technology/strain-gauge. [Accessed: 03-Jun-2015].

[19] F. E. Jones and R. M. Schoonover, *Handbook of Mass Measurement*. Hoboken, NJ: CRC Press, 2002.

[20] Y. Attikiouzel, "Dietetic measurement apparatus," U.S. Patent: 4911256, issued date Mar. 27, 1990.

[21] T. Yamazaki and T. Ono, "Dynamic Problems in Measurement of Mass-related Quantities," in *SICE Annual Conference, Kagawa University, Japan*, 2007.

[22] P. et al Pietrzak, "Dynamic mass measurement in checkweighers using a discrete time-variant low-pass filter," *Mech. Syst. Signal Process.*, no. 48, pp. 67–76, 2014.

[23] T. Ono, K. Kameoka, H. Sekiguchi, and K. Nakajima, "Studies on Dynamic Measurement Method of Mass and Weight (Part 3)," *JSME*, vol. 23, no. 185.

[24] T. Ono, K. Kameoka, H. Sekiguchi, and K. Nakajima, "Studies on Dynamic Measurement Method of Mass and Weight (Part 4)," *JSME*, vol. 24, no. 192, 1981.

[25] T. Ono, K. Kameoka, and K. Nakajima, "Studies on Dynamic Measurement Method of Mass and Weight (Part 2)," *JSME*, vol. 23, no. 177.

[26] U.S. Department of Transportation - Federal Highway Administration, "Commercial Vehicle Size and Weight Program," 2013. [Online]. Available: http://ops.fhwa.dot.gov/Freight/sw/overview/index.htm. [Accessed: 02-Jun-2015].

[27] N. US Department of Commerce, "National Institute of Standards and Technology Handbook 44," 2015. [Online]. Available: http://www.nist.gov/pml/wmd/pubs/hb44.cfm. [Accessed: 07-Jun-2015].

[28] R. Schwartz, "Automatic Weighing - Principles, Applications, and Developments," in *XVI IMEKO World Congress, Vienna, Austria*.

[29] M. J. Kranz, B. Sphatt, and M. J. Massey, "On-board truck scale," U.S. Patent: 20070181350 , issued date Aug. 9, 2007.

[30] G. R. Potts, “Methods and systems for dynamic force measurement,” U.S. Patent: 6606569, issued date Aug. 12, 2003.

[31] C. T. Kyrtsos and D. A. Worrell, “Dynamic payload monitor,” U.S. Patent: 4919222, issued date Apr 24, 1990.

[32] S. Ichiyama, Y. Aoyagi, and T. Yasuda, “Load weight indicating system for load moving machine,” U.S. Patent: 4627013, issued date Dec. 2, 1986.

ACKNOWLEDGEMENTS

I would like to take this opportunity to thank Dr. Vance for the guidance and support she provided me during graduate school. Throughout my research, her advice and encouragement helped me work through the obstacles and challenges of the project. I would like to thank Dr. Luecke for the support provided throughout my undergraduate studies, and the continued support into graduate school by serving as a committee member. I would also like to thank Dr. Steward for serving on my committee.

I would like to thank my family and friends for their continued support throughout my studies and thesis.